19

THE 1RSB CAVITY METHOD

The effectiveness of belief propagation depends on one basic assumption: when a function node is pruned from the factor graph, the adjacent variables become weakly correlated with respect to the resulting distribution. This hypothesis may break down either because of the existence of small loops in the factor graph, or because variables are correlated on large distances. In factor graphs with a locally tree-like structure, the second scenario is responsible for the failure of BP. The emergence of such long range correlations is a signature of a phase transition separating a 'weakly correlated' and a 'highly correlated' phase. The latter is often characterized by the decomposition of the (Boltzmann) probability distribution into well separated 'lumps' (pure Gibbs states).

We considered a simple example of this phenomenon in our study of random XORSAT. A similar scenario holds in a variety of problems from random graph coloring to random satisfiability and spin glasses. The reader should be warned that the structure and organization of pure states in such systems is far from being fully understood. Furthermore, the connection between long range correlations and pure states decomposition is more subtle than suggested by the above remarks.

Despite these complications, physicists have developed a non-rigorous approach to deal with this phenomenon: the "one step replica symmetry breaking" (1RSB) cavity method. The method postulates a few properties of the pure state decomposition, and, on this basis, allows to derive a number of quantitative predictions ('conjectures' from a mathematics point of view). Examples include the satisfiability threshold for random K-SAT and other random constraint satisfaction problems.

The method is rich enough to allow for some self-consistency checks of such assumptions. In several cases in which the 1RSB cavity method passed this test, its predictions have been confirmed by rigorous arguments (and there is no case in which they have been falsified so far). These successes encourage the quest for a mathematical theory of Gibbs states on sparse random graphs.

This chapter explains the 1RSB cavity method. It alternates between a general presentation and a concrete illustration on the XORSAT problem. We strongly encourage the reader to read the previous chapter on XORSAT before the present one. This should help her to gain some intuition of the whole scenario.

We start with a general description of the 1RSB glass phase, and the decomposition in pure states, in Sec. 19.1. Section 19.2 introduces an auxiliary constraint satisfaction problem to count the number of solutions of BP equations. The 1RSB analysis amounts to applying belief propagation to this auxil-

iary problem. One can then apply the methods of Ch. 14 (for instance, density evolution) to the auxiliary problem. Section 19.3 illustrates the approach on the XORSAT problem and shows how the 1RSB cavity method recovers the rigorous results of the previous chapter.

In Sec. 19.4 we show how the 1RSB formalism, which in general is rather complicated, simplifies considerably when the temperature of the auxiliary constraint satisfaction problem takes the value $\mathtt{x} = 1$. Section 19.5 explains how to apply it to optimization problems (leveraging on the min-sum algorithm) leading to the Survey Propagation algorithm. The concluding section 19.6 describes the physical intuition which underlies the whole method. The appendix 19.6.3 contains some technical aspects of the survey propagation equations applied to XORSAT, and their statistical analysis.

19.1 Beyond BP: many states

19.1.1 *Bethe measures*

The main lesson of the previous chapters is that in many cases, the probability distribution specified by graphical models with a locally tree-like structure takes a relatively simple form, that we shall call a Bethe measure (or Bethe state). Let us first define precisely what we mean by this, before we proceed to discuss what kinds of other scenarios can be encountered.

As in Ch. 14, we consider a factor graph $G = (V, F, E)$, with variable nodes $V = \{1, \cdots, N\}$, factor nodes $F = \{1, \cdots, M\}$ and edges E. The joint probability distribution over the variables $\underline{x} = (x_1, \dots, x_N) \in \mathcal{X}^N$ takes the form

$$\mu(\underline{x}) = \frac{1}{Z} \prod_{a=1}^{M} \psi_a(\underline{x}_{\partial a})\,. \tag{19.1}$$

Given a subset of variable nodes $U \subseteq V$ (which we shall call a 'cavity'), the **induced subgraph** $G_U = (U, F_U, E_U)$ is defined as the factor graph that includes all the factor nodes a such that $\partial a \subseteq U$, and the adjacent edges. We also write $(i, a) \in \partial U$ if $i \in U$ and $a \in F \setminus F_U$. Finally, a **set of messages** $\{\widehat{\nu}_{a\to i}\}$ is a set of probability distributions over $\mathcal{X}$, indexed by directed edges $a \to i$ in E with $a \in F$, $i \in V$.

Definition 19.1. (Informal) *The probability distribution μ is a **Bethe measure** (or **Bethe state**) if there exists a set of messages $\{\widehat{\nu}_{a\to i}\}$, such that, for 'almost all' the 'finite size' cavities U, the distribution $\mu_U(\,\cdot\,)$ of the variables in U is approximated as*

$$\mu_U(\underline{x}_U) \cong \prod_{a\in F_U} \psi_a(\underline{x}_{\partial a}) \prod_{(ia)\in\partial U} \widehat{\nu}_{a\to i}(x_i) \;+\; \mathsf{err}(\underline{x}_U)\,, \tag{19.2}$$

where $\mathsf{err}(\underline{x}_U)$ is a 'small' error term, and $\cong$ denotes as usual equality up to a normalization.

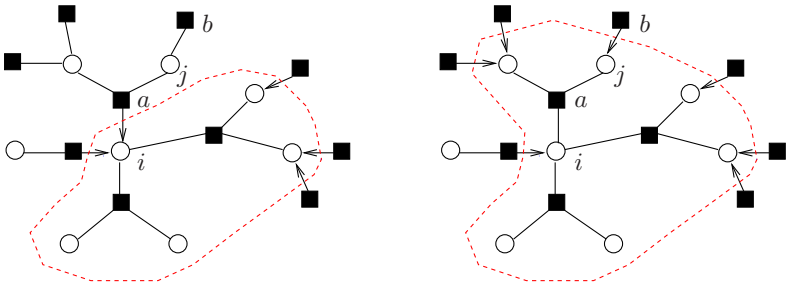

FIG. 19.1. Two examples of cavities. The right hand one is obtained by adding the extra function node a. The consistency of the Bethe measure in these two cavities implies the BP equation for $\widehat{\nu}_{a\to i}$, see Exercise 19.1.

A formal definition should specify what is meant by 'almost all', 'finite size' and 'small.' This can be done by introducing a tolerance ϵ_N (with $\epsilon_N \downarrow 0$ as $N \to \infty$) and a size L_N (where L_N is bounded as $N \to \infty$). One then requires that some norm of $\mathsf{err}(\,\cdot\,)$ (e.g. an L_p norm) is smaller than ϵ_N for a fraction larger than $1-\epsilon_N$ of all possible cavities U of size $|U| < L_N$. The underlying intuition is that the measure $\mu(\,\cdot\,)$ is well approximated locally by the given set of messages. In the following we shall follow physicists' habit of leaving implicit the various approximation errors.

Notice that the above definition does not make use of the fact that μ factorizes as in Eq. (19.1). It thus apply to any distribution over $\underline{x} = \{x_i : i \in V\}$.

If $\mu(\,\cdot\,)$ is a Bethe measure with respect to the message set $\{\widehat{\nu}_{a\to i}\}$, then the consistency of Eq. (19.2) for different choices of U implies some non-trivial constraints on the messages. In particular if the loops in the factor graph G are not too small (and under some technical condition on the functions $\psi_a(\,\cdot\,)$) then the messages must be close to satisfying BP equations. More precisely, we define a **quasi-solution** of BP equations as a set of messages which satisfy almost all the equations within some accuracy. The reader is invited to prove this statement in the exercise below.

Exercise 19.1 Assume that $G = (V, F, E)$ has girth larger than 2, and that $\mu(\,\cdot\,)$ is a Bethe measure with respect to the message set $\{\widehat{\nu}_{a\to i}\}$ where $\widehat{\nu}_{a\to i}(x_i) > 0$ for any $(i,a) \in E$, and $\psi_a(\underline{x}_{\partial a}) > 0$ for any $a \in F$. For $U \subseteq V$, and $(i,a) \in \partial U$, define a new subset of variable nodes as $W = U \cup \partial a$ (see Fig. 19.1).

Applying Eq. (19.2) to the subsets of variables U and W, show that the message must satisfy (up to an error term of the same order as $\mathsf{err}(\,\cdot\,)$):

$$\widehat{\nu}_{a\to i}(x_i) \cong \sum_{\underline{x}_{\partial a\setminus i}} \psi_a(\underline{x}_{\partial a}) \prod_{j\in\partial a\setminus i} \Big\{ \prod_{b\in\partial j\setminus a} \widehat{\nu}_{b\to j}(x_j) \Big\} . \tag{19.3}$$

Show that these are equivalent to the BP equations (14.14), (14.15).
[Hint: Define, for $k \in V$, $c \in F$, $(k,c) \in E$, $\nu_{k\to c}(x_k) \cong \prod_{d\in\partial k\setminus c} \widehat{\nu}_{d\to k}(x_k)$].

It would be pleasant if the converse was true, i.e. if each quasi-solution of BP equations corresponded to a distinct Bethe measure. In fact such a relation will be at the heart of the assumptions of the 1RSB method. However one should keep in mind that this is not always true, as the following example shows:

Example 19.2 Let G be a factor graph with the same degree $K \geq 3$ both at factor and variable nodes. Consider binary variables, $\mathcal{X} = \{0, 1\}$, and, for each $a \in F$, let

$$\psi_a(x_{i_1(a)}, \dots, x_{i_K(a)}) = \mathbb{I}(x_{i_1(a)} \oplus \cdots \oplus x_{i_K(a)} = 0) . \tag{19.4}$$

Given a perfect matching $\mathsf{M} \subseteq E$, a solution of BP equations can be constructed as follows. If $(i,a) \in \mathsf{M}$, then let $\widehat{\nu}_{a\to i}(x_i) = \mathbb{I}(x_i = 0)$ and $\nu_{i\to a}(0) = \nu_{i\to a}(1) = 1/2$. If on the other hand $(i,a) \notin \mathsf{M}$, then let $\widehat{\nu}_{a\to i}(0) = \widehat{\nu}_{a\to i}(1) = 1/2$ and $\nu_{i\to a}(0) = \mathbb{I}(x_i = 0)$ (variable to factor node).

Check that this is a solution of BP equations and that all the resulting local marginals coincide with the ones of the measure $\mu(\underline{x}) \cong \mathbb{I}(\underline{x} = \underline{0})$, independently of M. If one takes for instance G to be a random regular graph with degree $K \geq 3$, both at factor nodes and variable nodes, then the number of perfect matchings of G is, with high probability, exponential in the number of nodes. Therefore we have constructed an exponential number of solutions of BP equations that describe the same Bethe measure.

19.1.2 *A few generic scenarios*

Bethe measures are a conceptual tool for describing distributions of the form (19.1). Inspired by the study of glassy phases (see Sec. 12.3), statistical mechanics studies have singled out a few generic scenarios in this respect, that we informally describe below.

RS (replica symmetric). This is the simplest possible scenario: the distribution $\mu(\,\cdot\,)$ is a Bethe measure.

A slightly more complicated situation (that we still ascribe to the 'replica symmetric' family) arises when $\mu(\,\cdot\,)$ decomposes into a finite set of Bethe measures related by 'global symmetries', as in the Ising ferromagnet discussed in Sec. 17.3.

d1RSB (dynamic one-step replica symmetry breaking). There exists an exponentially large (in the system size N) number of Bethe measures. The measure μ decomposes into a convex combination of these Bethe measures:

$$\mu(\underline{x}) = \sum_n w_n \, \mu^n(\underline{x}) \,, \tag{19.5}$$

with weights w_n exponentially small in N. Furthermore $\mu(\,\cdot\,)$ is itself a Bethe measure.

s1RSB (static one-step replica symmetry breaking). As in the d1RSB case, there exists an exponential number of Bethe measures, and μ decomposes into a convex combination of such states. However, a finite number of the weights w_n is of order 1 as $N \to \infty$, and (unlike in the previous case) μ is not itself a Bethe measure.

In the following we shall focus on the d1RSB and s1RSB scenarios, that are particularly interesting, and can be treated in a unified framework (we shall sometimes refer to both of them as 1RSB). More complicate scenarios, such as 'full RSB', are also possible. We do not discuss such scenarios here because, so far, one has a relatively poor control of them in sparse graphical models.

In order to proceed further, we shall make a series of assumptions on the structure of Bethe states in the 1RSB case. While further research work is required to formalize completely these assumptions, they are precise enough for deriving several interesting quantitative predictions.

To avoid technical complications, we assume that the compatibility functions $\psi_a(\,\cdot\,)$ are strictly positive. (The cases with $\psi_a(\,\cdot\,) = 0$ should be treated as limit cases of such models). Let us index by n the various quasi-solutions $\{\nu^n_{i\to a}, \widehat{\nu}^n_{a\to i}\}$ of the BP equations. To each of them we can associate a Bethe measure, and we can compute the corresponding Bethe free-entropy $\mathbb{F}_n = \mathbb{F}(\underline{\nu}^n)$. The three postulates of the 1RSB scenario are listed below.

Assumption 1 *There exist exponentially many quasi-solutions of BP equations. The number of such solutions with free-entropy $\mathbb{F}(\underline{\nu}^n) \approx N\phi$ is (to leading exponential order)* $\exp\{N\Sigma(\phi)\}$*, where $\Sigma(\,\cdot\,)$ is the* ***complexity*** *function*[27] .

This can be expressed more formally as follows. There exists a function $\Sigma : \mathbb{R} \to \mathbb{R}_+$ (the complexity) such that, for any interval $[\phi_1, \phi_2]$, the number of quasi-solutions of BP equations with $\mathbb{F}(\underline{\nu}^n) \in [N\phi_1, N\phi_2]$ is $\exp\{N\Sigma_* + o(N)\}$ where $\Sigma_* = \sup\{\Sigma(\phi) : \quad \phi_1 \le \phi \le \phi_2\}$. We shall also assume in the following that $\Sigma(\phi)$ is 'regular enough' without entering details.

[27] As we are only interested in the leading exponential behavior, the details of the definitions of quasi-solutions become irrelevant, as long as (for instance) the fraction of violated BP equations vanishes in the large N limit.

Among Bethe measures, a special role is played by the ones that have short range correlations (are *extremal*). We already mentioned this point in Ch. 12, and shall discuss the relevant notion of correlation decay in Ch. 22. We denote the set of extremal measures as E.

Assumption 2 *The 'canonical' measure μ defined as in Eq. (19.1) can be written as a convex combination of extremal Bethe measures*

$$\mu(\underline{x}) = \sum_{n\in\mathsf{E}} w_n\, \mu^n(\underline{x}) \ , \tag{19.6}$$

with weights related to the Bethe free-entropies $w_n = e^{\mathbb{F}_n}/\Xi$, $\Xi \equiv \sum_{n\in\mathsf{E}} e^{\mathbb{F}_n}$.

Note that Assumption 1 characterizes the number of (approximate) BP fixed points, while Assumption 2 expresses the measure $\mu(\,\cdot\,)$ in terms of extremal Bethe measures. While each such measure gives rise to a BP fixed point by the arguments in the previous Section, it is not clear that the reciprocal holds. The next assumption implies that this is the case, to the leading exponential order.

Assumption 3 *To leading exponential order, the number of extremal Bethe measures equals the number of quasi-solutions of BP equation: the number of extremal Bethe measures with free-entropy $\approx N\phi$ is also given by* $\exp\{N\Sigma(\phi)\}$.

19.2 The 1RSB cavity equations

Within the three assumptions described above, the complexity function $\Sigma(\phi)$ provides basic information on how the measure μ decomposes into Bethe measures. Since the number of extremal Bethe measures with a given free entropy density is exponential in the system size, it is natural to treat them within a statistical physics formalism. BP messages of the original problem will be the new variables and Bethe measures will be the new configurations. This is what 1RSB is about.

We introduce the auxiliary statistical physics problem through the definition of a canonical distribution over extremal Bethe measures: we assign to measure $n \in \mathsf{E}$, the probability $w_n(\mathtt{x}) = e^{\mathtt{x}\mathbb{F}_n}/\Xi(\mathtt{x})$. Here $\mathtt{x}$ plays the role of an inverse temperature (and is often called the **Parisi 1RSB parameter**) [28]. The partition function of this generalized problem is

$$\Xi(\mathtt{x}) = \sum_{n\in\mathsf{E}} e^{\mathtt{x}\mathbb{F}_n} \doteq \int e^{N[\mathtt{x}\phi+\Sigma(\phi)]}\, \mathrm{d}\phi\,. \tag{19.7}$$

According to Assumption 2 above, extremal Bethe measures contribute to μ through a weight $w_n = e^{\mathbb{F}_n}/\Xi$. Therefore the original problem is described by the choice $\mathtt{x} = 1$. But varying $\mathtt{x}$ will allow us to recover the full complexity function $\Sigma(\phi)$.

[28] It turns out that the present approach is equivalent the cloning method discussed in Chapter 12, where $\mathtt{x}$ is the number of clones.

If $\Xi(\mathtt{x}) \doteq e^{N\mathfrak{F}(\mathtt{x})}$, a saddle point evaluation of the integral in (19.7) gives Σ as the Legendre transform of $\mathfrak{F}$:

$$\mathfrak{F}(\mathtt{x}) = \mathtt{x}\phi + \Sigma(\phi)\,, \qquad \frac{\partial\Sigma}{\partial\phi} = -\mathtt{x}\ . \tag{19.8}$$

19.2.1 *Counting BP fixed points*

In order to actually estimate $\Xi(\mathtt{x})$, we need to consider the distribution induced by $w_n(\mathtt{x})$ on the messages $\underline{\nu} = \{\nu_{i\to a}, \widehat{\nu}_{a\to i}\}$, that we shall denote by $\mathsf{P}_x(\underline{\nu})$. The fundamental observation is that this distribution can be written as a graphical model, whose variables are BP messages. A first family of function nodes enforces the BP equations, and a second one implements the weight $e^{\mathtt{x}\mathbb{F}(\underline{\nu})}$. Furthermore, it turns out that the topology of the factor graph in this **auxiliary graphical model** is very close to that of the original factor graph. This suggests to use the BP approximation in this auxiliary model in order to estimate $\Sigma(\phi)$.

The 1RSB approach can be therefore summarized in one sentence:

Introduce a Boltzmann distribution over Bethe measures, write it in the form of a graphical model, and use BP to study this model.

This program is straightforward, but one must be careful not to confuse the two models (the original one and the auxiliary one), and their messages. Let us first simplify the notations of the original messages. The two types of messages entering the BP equations of the original problem will be denoted by $\widehat{\nu}_{a\to i} = \widehat{\mathtt{m}}_{ai}$ and $\nu_{i\to a} = \mathtt{m}_{ia}$; we will denote by $\underline{\mathtt{m}}$ the set of all the $\mathtt{m}_{ia}$ and by $\underline{\widehat{\mathtt{m}}}$ the set of all the $\widehat{\mathtt{m}}_{ai}$. Each of these $2|\mathcal{E}|$ messages is a normalized probability distribution over the alphabet $\mathcal{X}$. With these notations, the original BP equations read:

$$\mathtt{m}_{ia}(x_i) \cong \prod_{b\in\partial i\setminus a} \widehat{\mathtt{m}}_{bi}(x_i)\,, \qquad \widehat{\mathtt{m}}_{ai}(x_i) \cong \sum_{\{x_j\}_{j\in\partial a\setminus i}} \psi_a(\underline{x}_{\partial a}) \prod_{j\in\partial a\setminus i} \mathtt{m}_{ja}(x_j)\,. \tag{19.9}$$

Hereafter we shall write them in the compact form:

$$\mathtt{m}_{ia} = \mathsf{f}_i\left(\{\widehat{\mathtt{m}}_{bi}\}_{b\in\partial i\setminus a}\right)\,, \qquad \widehat{\mathtt{m}}_{ai} = \hat{\mathsf{f}}_a\left(\{\mathtt{m}_{ja}\}_{j\in\partial a\setminus i}\right)\ . \tag{19.10}$$

Each message set $(\underline{\mathtt{m}}, \underline{\widehat{\mathtt{m}}})$ is given a weight proportional to $e^{\mathtt{x}\mathbb{F}(\underline{\mathtt{m}},\underline{\widehat{\mathtt{m}}})}$, where the free-entropy $\mathbb{F}(\underline{\mathtt{m}}, \underline{\widehat{\mathtt{m}}})$ is written in terms of BP messages

$$\mathbb{F}(\underline{\mathtt{m}}, \underline{\widehat{\mathtt{m}}}) = \sum_{a\in F}\mathbb{F}_a\left(\{\mathtt{m}_{ja}\}_{j\in\partial a}\right) + \sum_{i\in V}\mathbb{F}_i\left(\{\widehat{\mathtt{m}}_{bi}\}_{b\in\partial i}\right) - \sum_{(ia)\in E}\mathbb{F}_{ia}\left(\mathtt{m}_{ia}, \widehat{\mathtt{m}}_{ai}\right)\ . \tag{19.11}$$

The functions $\mathbb{F}_a, \mathbb{F}_i, \mathbb{F}_{ia}$ have been obtained in (14.28). Let us copy them here for convenience:

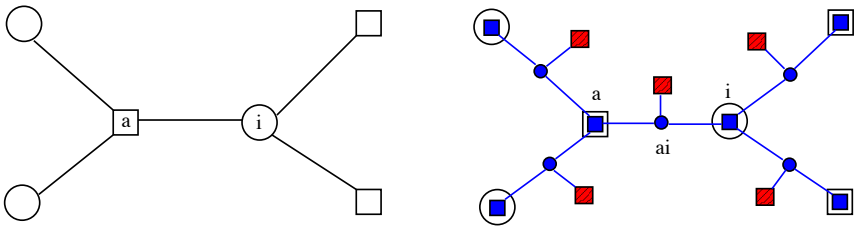

FIG. 19.2. A part of the original factor graph (left) and the corresponding auxiliary factor graph (right)

$$\mathbb{F}_a(\{\mathtt{m}_{ja}\}_{j\in\partial a}) = \log\left[\sum_{\underline{x}_{\partial a}} \psi_a(\underline{x}_{\partial a}) \prod_{j\in\partial a} \mathtt{m}_{ja}(x_j)\right] ,$$

$$\mathbb{F}_i(\{\widehat{\mathtt{m}}_{bi}\}_{b\in\partial i}) = \log\left[\sum_{x_i} \prod_{b\in\partial i} \widehat{\mathtt{m}}_{bi}(x_i)\right] , \tag{19.12}$$

$$\mathbb{F}_{ia}(\mathtt{m}_{ia}, \widehat{\mathtt{m}}_{ai}) = \log\left[\sum_{x_i} \mathtt{m}_{ia}(x_i)\widehat{\mathtt{m}}_{ai}(x_i)\right] . \tag{19.13}$$

We now consider the $2|\mathcal{E}|$ messages $\underline{\mathtt{m}}$ and $\underline{\widehat{\mathtt{m}}}$ as variables in our auxiliary graphical model. The distribution induced my $w_n(\mathtt{x})$ on such messages takes the form

$$\mathsf{P}_{\mathtt{x}}(\underline{\mathtt{m}}, \underline{\widehat{\mathtt{m}}}) = \frac{1}{\Xi(x)} \prod_{a\in F} \Psi_a(\{\mathtt{m}_{ja}, \widehat{\mathtt{m}}_{ja}\}_{j\in\partial a}) \prod_{i\in V} \Psi_i(\{\mathtt{m}_{ib}, \widehat{\mathtt{m}}_{ib}\}_{b\in\partial i}) \prod_{(ia)\in E} \Psi_{ia}(\mathtt{m}_{ia}, \widehat{\mathtt{m}}_{ia}) , \tag{19.14}$$

where we introduced the compatibility functions:

$$\Psi_a = \prod_{i\in\partial a} \mathbb{I}\left(\widehat{\mathtt{m}}_{ai} = \hat{\mathsf{f}}_a\left(\{\mathtt{m}_{ja}\}_{j\in\partial a\setminus i}\right)\right) \quad e^{\mathtt{x}\mathbb{F}_a(\{\mathtt{m}_{ja}\}_{j\in\partial a})} , \tag{19.15}$$

$$\Psi_i = \prod_{a\in\partial i} \mathbb{I}\left(\mathtt{m}_{ia} = \mathsf{f}_i\left(\{\widehat{\mathtt{m}}_{bi}\}_{b\in\partial i\setminus a}\right)\right) \quad e^{\mathtt{x}\mathbb{F}_i(\{\widehat{\mathtt{m}}_{bi}\}_{b\in\partial i})} , \tag{19.16}$$

$$\Psi_{ia} = e^{-\mathtt{x}\mathbb{F}_{ia}(\mathtt{m}_{ia}, \widehat{\mathtt{m}}_{ai})} . \tag{19.17}$$

The corresponding factor graph is depicted in Fig. 19.2 and can described as follows:

- *For each edge* (i, a) *of the original factor graph*, introduce a variable node in the auxiliary factor graph. The associated variable is the pair $(\mathtt{m}_{ia}, \widehat{\mathtt{m}}_{ai})$. Furthermore, introduce a function node connected to this variable, contributing to the weight through a factor $\Psi_{ia} = e^{-\mathtt{x}\mathbb{F}_{ai}}$.
- *For each function node* a *of the original graph* introduce a function node in the auxiliary graph and connect it to all the variable nodes corresponding

to edges (i,a), $i \in \partial a$. The compatibility function Ψ_a associated to this function node has two roles: (i) It enforces the $|\partial a|$ BP equations expressing the variables $\{\widehat{\mathtt{m}}_{ai}\}_{i\in\partial a}$ in terms of the $\{\mathtt{m}_{ia}\}_{i\in\partial a}$, cf. Eq. (19.9); (ii) It contributes to the weight through a factor $e^{\mathtt{x}\mathbb{F}_a}$.

- *For each variable node i of the original graph*, introduce a function node in the auxiliary graph, and connect it to all variable nodes corresponding to edges (i,a), $a \in \partial i$. The compatibility function Ψ_i has two roles: (i) It enforces the $|\partial i|$ BP equations expressing the variables $\{\mathtt{m}_{ib}\}_{b\in\partial i}$ in terms of $\{\widehat{\mathtt{m}}_{bi}\}_{b\in\partial i}$, cf. Eq. (19.9); (ii) It contributes to the weight through a factor $e^{\mathtt{x}\mathbb{F}_i}$.

Note that we were a bit sloppy in Eqs. (19.15) to (19.17). The messages $\mathtt{m}_{ia}$, $\widehat{\mathtt{m}}_{ai}$ are in general continuous, and indicator functions should therefore be replaced by delta functions. This might pose in turn some definition problem (what is the reference measure on the messages? can we hope for *exact* solutions of BP equations?). One should consider the above as a shorthand for the following procedure. First discretize the messages (and BP equations) in such a way that they can take a finite number q of values. Compute the complexity by letting $N \to \infty$ at fixed q, and take the limit $q \to \infty$ at the end. It is easy to define several alternative, and equally reasonable, limiting procedures. We expect all of them to yield the same result. In practice, the ambiguities in Eqs. (19.15) to (19.17) are solved on a case by case basis.

19.2.2 *Message passing on the auxiliary model*

The problem of counting the number of Bethe measures (more precisely, computing the complexity function $\Sigma(\phi)$) has been reduced to the one of estimating the partition function $\Xi(\mathtt{x})$ of the auxiliary graphical model (19.14). Since we are interested in the case of locally tree-like factor graphs G, the auxiliary factor graph is locally tree-like as well. We can therefore apply BP to estimate its free-entropy density $\mathfrak{F}(\mathtt{x}) = \lim_N N^{-1}\log\Xi(\mathtt{x})$. This will give us the complexity through the Legendre transform of Eq. (19.8).

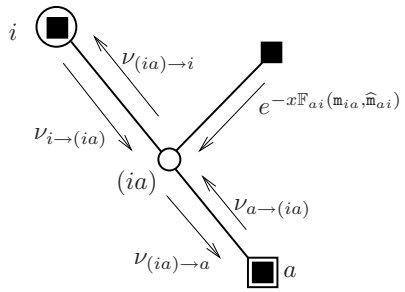

FIG. 19.3. Messages in the auxiliary graphical model.

In the following we denote by $i \in V$ and $a \in F$ a generic variable and function

node in the graph G, and by $(ia) \in E$ an edge in G. By extension, we denote in the same way the corresponding nodes in the auxiliary graph. The messages appearing in the BP analysis of the auxiliary model can be classified as follows, cf. Fig. 19.3:

- → From the variable node (ia) are issued two messages: $\nu_{(ia)\to a}(\mathtt{m}_{ia}, \widehat{\mathtt{m}}_{ai})$ and $\nu_{(ia)\to i}(\mathtt{m}_{ia}, \widehat{\mathtt{m}}_{ai})$
- → From the function node a are issued $|\partial a|$ messages to nodes $i \in \partial a$, $\widehat{\nu}_{a\to(ai)}(\mathtt{m}_{ia}, \widehat{\mathtt{m}}_{ai})$
- → From the function node i are issued $|\partial i|$ messages to nodes $a \in \partial i$, $\widehat{\nu}_{i\to(ai)}(\mathtt{m}_{ia}, \widehat{\mathtt{m}}_{ai})$
- → From the degree-one function node connected to the variable node (ia) is issued a message towards this variable. This message is simply $e^{-\mathtt{x}\mathbb{F}_{ia}(\mathtt{m}_{ia}, \widehat{\mathtt{m}}_{ai})}$.

The BP equations on the variable node (ia) take a simple form:

$$\begin{aligned}\nu_{(ia)\to a}(\mathtt{m}_{ia}, \widehat{\mathtt{m}}_{ai}) &\cong \widehat{\nu}_{i\to(ia)}(\mathtt{m}_{ia}, \widehat{\mathtt{m}}_{ai})\; e^{-\mathtt{x}\mathbb{F}_{ia}(\mathtt{m}_{ia}, \widehat{\mathtt{m}}_{ai})}\,,\\ \nu_{(ia)\to i}(\mathtt{m}_{ia}, \widehat{\mathtt{m}}_{ai}) &\cong \widehat{\nu}_{a\to(ia)}(\mathtt{m}_{ia}, \widehat{\mathtt{m}}_{ai})\; e^{-\mathtt{x}\mathbb{F}_{ia}(\mathtt{m}_{ia}, \widehat{\mathtt{m}}_{ai})}\,. \end{aligned} \tag{19.18}$$

We can use these equations to eliminate messages $\widehat{\nu}_{i\to(ia)}$, $\widehat{\nu}_{a\to(ia)}$ in favor of $\nu_{(ia)\to a}$, $\nu_{(ia)\to i}$. In order to emphasize this choice (and to simplify notations) we define:

$$Q_{ia}(\mathtt{m}_{ia}, \widehat{\mathtt{m}}_{ai}) \equiv \nu_{(ia)\to a}(\mathtt{m}_{ia}, \widehat{\mathtt{m}}_{ai})\,, \qquad \widehat{Q}_{ai}(\mathtt{m}_{ia}, \widehat{\mathtt{m}}_{ai}) \equiv \nu_{(ia)\to i}(\mathtt{m}_{ia}, \widehat{\mathtt{m}}_{ai})\,. \tag{19.19}$$

We can now write the remaining BP equations of the auxiliary graphical model in terms of $Q_{ia}(\,\cdot\,,\,\cdot\,)$, $\widehat{Q}_{ai}(\,\cdot\,,\,\cdot\,)$. The BP equation associated to the function node corresponding to $i \in V$ reads:

$$\begin{aligned} Q_{ia}(\mathtt{m}_{ia}, \widehat{\mathtt{m}}_{ai}) \cong \sum_{\{\mathtt{m}_{ib}, \widehat{\mathtt{m}}_{bi}\}_{b\in\partial i\setminus a}} &\left[\prod_{c\in\partial i} \mathbb{I}\left(\mathtt{m}_{ic} = \mathsf{f}_i(\{\widehat{\mathtt{m}}_{di}\}_{d\in\partial i\setminus c})\right)\right] \\ &\exp\left\{\mathtt{x}\left[\mathbb{F}_i\left(\{\widehat{\mathtt{m}}_{bi}\}_{b\in\partial i}\right) - \mathbb{F}_{ai}\left(\mathtt{m}_{ia}, \widehat{\mathtt{m}}_{ai}\right)\right]\right\} \prod_{b\in\partial i\setminus a} \widehat{Q}_{bi}(\mathtt{m}_{ib}, \widehat{\mathtt{m}}_{bi})\,, \end{aligned} \tag{19.20}$$

and the one associated to the function node corresponding to $a \in F$ is:

$$\widehat{Q}_{ai}(\mathtt{m}_{ia}, \widehat{\mathtt{m}}_{ai}) \cong \sum_{\{\mathtt{m}_{ja}, \widehat{\mathtt{m}}_{aj}\}_{j\in\partial a\setminus i}} \left[\prod_{j\in\partial a} \mathbb{I}\left(\widehat{\mathtt{m}}_{aj} = \hat{\mathsf{f}}_a(\{\mathtt{m}_{ka}\}_{k\in\partial a\setminus j})\right)\right] \tag{19.21}$$

$$\exp\left\{\mathtt{x}\left[\mathbb{F}_a\left(\{\mathtt{m}_{ja}\}_{j\in\partial a}\right\} - \mathbb{F}_{ai}\left(\mathtt{m}_{ia}, \widehat{\mathtt{m}}_{ai}\right)\right]\right) \prod_{j\in\partial a\setminus i} Q_{ja}(\mathtt{m}_{ja}, \widehat{\mathtt{m}}_{aj})\,. \tag{19.22}$$

Equations (19.20), (19.22) can be further simplified, using the following lemma.

Lemma 19.3 *Assume* $\sum_{x_i} \mathtt{m}_{ia}(x_i)\widehat{\mathtt{m}}_{ai}(x_i) > 0$. *Under the condition* $\mathtt{m}_{ia} = \mathsf{f}_i(\{\widehat{\mathtt{m}}_{di}\}_{d\in\partial i\setminus a})$ *(in particular if the indicator functions in Eq. (19.20) evaluate to* 1*), the difference* $\mathbb{F}_i(\{\widehat{\mathtt{m}}_{bi}\}_{b\in\partial i}) - \mathbb{F}_{ai}(\mathtt{m}_{ia}, \widehat{\mathtt{m}}_{ai})$ *can be expressed in terms of* $\{\widehat{\mathtt{m}}_{bi}\}_{b\in\partial i\setminus a}$. *Explicitly, we have*

$$e^{\mathbb{F}_i - \mathbb{F}_{ia}} = z_{ia}(\{\widehat{\mathtt{m}}_{bi}\}_{b\in\partial i\setminus a}) \equiv \sum_{x_i} \prod_{b\in\partial i\setminus a} \widehat{\mathtt{m}}_{bi}(x_i)\,. \tag{19.23}$$

Analogously, under the condition $\widehat{\mathtt{m}}_{ai} = \hat{\mathsf{f}}_a(\{\mathtt{m}_{ka}\}_{k\in\partial a\setminus i})$ *(in particular if the indicator functions in Eq. (19.22) evaluate to* 1*) the difference* $\mathbb{F}_a(\{\mathtt{m}_{ja}\}_{j\in\partial a}) - \mathbb{F}_{ai}(\mathtt{m}_{ia}, \widehat{\mathtt{m}}_{ai})$ *depends only on* $\{\mathtt{m}_{ja}\}_{j\in\partial a\setminus i}$. *Explicitly:*

$$e^{\mathbb{F}_a - \mathbb{F}_{ia}} = \hat{z}_{ai}(\{\mathtt{m}_{ja}\}_{j\in\partial a\setminus i}) \equiv \sum_{\underline{x}_{\partial a}} \psi_a(\underline{x}_{\partial a}) \prod_{j\in\partial a\setminus i} \mathtt{m}_{ja}(x_j)\,. \tag{19.24}$$

Proof: Let us first consider Eq. (19.23). From the definition (14.28), it follows that

$$e^{\mathbb{F}_i - \mathbb{F}_{ia}} = \frac{\sum_{x_i}\prod_{b\in\partial i}\widehat{\mathtt{m}}_{bi}(x_i)}{\sum_{x_i}\mathtt{m}_{ia}(x_i)\widehat{\mathtt{m}}_{ai}(x_i)}\,. \tag{19.25}$$

Substituting $\mathtt{m}_{ia} = f_i(\{\widehat{\mathtt{m}}_{ci}\}_{c\in\partial i\setminus a})$ in the denominator, and keeping track of the normalization constant, we get

$$\sum_{x_i}\mathtt{m}_{ia}(x_i)\widehat{\mathtt{m}}_{ai}(x_i) = \frac{\sum_{x_i}\prod_{b\in\partial i}\widehat{\mathtt{m}}_{bi}(x_i)}{\sum_{x_i}\prod_{b\in\partial i\setminus a}\widehat{\mathtt{m}}_{ai}(x_i)}\,, \tag{19.26}$$

which implies Eq. (19.23).

The derivation of Eq. (19.24) is completely analogous and left as an exercise for the reader. □

Notice that the functions $z_{ia}(\,\cdot\,)$, $\hat{z}_{ai}(\,\cdot\,)$ appearing in Eqs. (19.23), (19.24) are in fact the normalization constants hidden by the $\cong$ notation in Eqs. (19.9).

Because of this lemma, we can seek a solution of Eqs. (19.20), (19.22) with Q_{ia} depending only on $\mathtt{m}_{ia}$, and $\widehat{Q}_{ai}$ depends only on $\widehat{\mathtt{m}}_{ai}$. Hereafter we shall focus on this case, and, with an abuse of notation, we shall write:

$$Q_{ia}(\mathtt{m}_{ia}, \widehat{\mathtt{m}}_{ai}) = Q_{ia}(\mathtt{m}_{ia})\,, \quad \widehat{Q}_{ia}(\mathtt{m}_{ia}, \widehat{\mathtt{m}}_{ai}) = \widehat{Q}_{ai}(\widehat{\mathtt{m}}_{ai})\,. \tag{19.27}$$

The BP equations for the auxiliary graphical model (19.20), (19.22) then become:

$$Q_{ia}(\mathtt{m}_{ia}) \cong \sum_{\{\widehat{\mathtt{m}}_{bi}\}} \mathbb{I}\left(\mathtt{m}_{ia} = g_i(\{\widehat{\mathtt{m}}_{bi}\})\right)\; [z_{ia}(\{\widehat{\mathtt{m}}_{bi}\})]^{\mathtt{x}} \prod_{b\in\partial i\setminus a} \widehat{Q}_{bi}(\widehat{\mathtt{m}}_{bi})\,, \tag{19.28}$$

$$\widehat{Q}_{ai}(\widehat{\mathtt{m}}_{ai}) \cong \sum_{\{\mathtt{m}_{ja}\}} \mathbb{I}\left(\widehat{\mathtt{m}}_{ai} = f_a(\{\mathtt{m}_{ja}\})\right)\; [\hat{z}_{ai}(\{\mathtt{m}_{ja}\})]^{\mathtt{x}} \prod_{j\in\partial a\setminus i} Q_{ja}(\mathtt{m}_{ja})\,, \tag{19.29}$$

where $\{\widehat{\mathtt{m}}_{bi}\}$ is a shorthand for $\{\widehat{\mathtt{m}}_{bi}\}_{b\in\partial i\setminus a}$ and $\{\mathtt{m}_{ja}\}$ a shorthand for $\{\mathtt{m}_{ja}\}_{j\in\partial a\setminus i}$. The expressions for $z_{ia}(\{\widehat{\mathtt{m}}_{bi}\})$ and $\hat{z}_{ai}(\{\mathtt{m}_{ja}\})$ are given in Eqs. (19.23), (19.24).

Equations (19.28), (19.29) are the **1RSB cavity equations**. As we did in the ordinary BP equations, we can consider them as an update rule for a message passing algorithm. This will be further discussed in the next sections. One sometimes uses the notation $Q_{i\to a}(\,\cdot\,)$, $\widehat{Q}_{a\to i}(\,\cdot\,)$, to emphasize the fact that 1RSB messages are associated to *directed* edges.

Notice that our derivation was based on the assumption that $\sum_{x_i} \mathtt{m}_{ia}(x_i)\widehat{\mathtt{m}}_{ai}(x_i) > 0$. This condition holds if, for instance, the compatibility functions of the original model are bounded away from 0. Under this condition, we have shown that:

Proposition 19.4 *If the 1RSB cavity equations (19.28), (19.29) have a solution $\widehat{Q}, Q$, this corresponds to a solution to the BP equations of the auxiliary graphical model. Reciprocally, if the BP equations of the auxiliary graphical model admit a solution satisfying the condition (19.27), then the resulting messages must be a solution of the 1RSB cavity equations.*

Assumption (19.27) -which is suggestive of a form of "causality"- cannot be further justified within the present approach, but alternative derivations of the 1RSB equations confirm its validity.

19.2.3 *Computing the complexity*

We now compute the free-entropy of the auxiliary graphical model within the BP approximation. We expect the result of this procedure to be asymptotically exact for a wide class of locally tree like graphs, thus yielding the correct free-entropy density $\mathfrak{F}(\mathtt{x}) = \lim_N N^{-1}\log\Xi(\mathtt{x})$.

Assume $\{Q_{ia}, \widehat{Q}_{ai}\}$ to be a solution (or a quasi-solution) of the 1RSB cavity equations (19.28), (19.29). We use the general form (14.27) of Bethe free-entropy, but take into account the degree one factor nodes using the simplified expression derived in Exercise 14.6. The various contributions to the free-entropy are:

→ Contribution from the function node a (here $\{\mathtt{m}_{ia}\}$ is a shorthand for $\{\mathtt{m}_{ia}\}_{i\in\partial a}$):

$$\mathbb{F}_a^{\rm RSB} = \log\left\{\sum_{\{\mathtt{m}_{ia}\}} e^{\mathtt{x}\mathbb{F}_a(\{\mathtt{m}_{ia}\})}\prod_{i\in\partial a} Q_{ia}(\mathtt{m}_{ia})\right\}. \tag{19.30}$$

→ Contribution from the function node i ($\{\widehat{\mathtt{m}}_{ai}\}$ is a shorthand for $\{\widehat{\mathtt{m}}_{ai}\}_{a\in\partial i}$):

$$\mathbb{F}_i^{\rm RSB} = \log\left\{\sum_{\{\widehat{\mathtt{m}}_{ai}\}} e^{\mathtt{x}\mathbb{F}_i(\{\widehat{\mathtt{m}}_{ai}\})}\prod_{a\in\partial i} \widehat{Q}_{ai}(\widehat{\mathtt{m}}_{ai})\right\}. \tag{19.31}$$

→ Contribution from the variable node (ia):

$$\mathbb{F}_{ia}^{\rm RSB} = \log\left\{\sum_{\mathtt{m}_{ia},\widehat{\mathtt{m}}_{ai}} e^{\mathtt{x}\mathbb{F}_{ia}(\mathtt{m}_{ia},\widehat{\mathtt{m}}_{ai})} Q_{ia}(\mathtt{m}_{ia})\widehat{Q}_{ai}(\widehat{\mathtt{m}}_{ai})\right\}. \tag{19.32}$$

→ The contributions from the two edges $a-(ai)$ and $i-(ai)$ are both equal to $-\mathbb{F}^{\rm RSB}_{ia}$

The Bethe free-entropy of the auxiliary graphical model is equal to:

$$\mathbb{F}^{\rm RSB}(\{Q,\widehat{Q}\}) = \sum_{a\in F}\mathbb{F}^{\rm RSB}_a + \sum_{i\in V}\mathbb{F}^{\rm RSB}_i - \sum_{(ia)\in E}\mathbb{F}^{\rm RSB}_{ia}\,. \tag{19.33}$$

19.2.4 *Summary*

The 1RSB cavity equations (19.28), (19.29) are BP equations for the auxiliary graphical model defined in (19.14). They relate $2|\mathcal{E}|$ messages $\{Q_{ia}(\mathtt{m}_{ia}),\ \widehat{Q}_{ai}(\widehat{\mathtt{m}}_{ai})\}$. Each such message is a probability distribution of ordinary BP messages, respectively $\mathtt{m}_{ia}(x_i)$ and $\widehat{\mathtt{m}}_{ai}(x_i)$. These elementary messages are in turn probability distributions on variables $x_i\in\mathcal{X}$.

Given a solution (or an approximate solution) $\{Q_{ia},\ \widehat{Q}_{ai}\}$, one can estimate the free-entropy density of the auxiliary model as

$$\log\Xi(\mathtt{x}) = \mathbb{F}^{\rm RSB}(\{Q,\widehat{Q}\}) + \mathsf{err}_N\,. \tag{19.34}$$

where $\mathbb{F}^{\rm RSB}(\{Q,\widehat{Q}\})$ is given by Eq. (19.33). For a large class of locally tree-like models we expect the BP approximation to be asymptotically exact on the auxiliary model. This means that the error term err_N is $o(N)$.

For such models, the free-entropy density is given by its 1RSB cavity expression $\mathfrak{F}(\mathtt{x}) = \mathrm{f}^{\rm RSB}(\mathtt{x}) \equiv \lim_{N\to\infty}\mathbb{F}^{\rm RSB}(\{Q,\widehat{Q}\})/N$. The complexity $\Sigma(\phi)$ is then computed through the Legendre transform (19.8).

19.2.5 *Random graphical models and density evolution*

Let us consider the case where G is a random graphical model as defined in Sec. 14.6.1. The factor graph is distributed according to one of the ensembles $\mathbb{G}_N(K,\alpha)$ or $\mathbb{D}_N(\Lambda,P)$. Function nodes are taken from a finite list $\{\psi^{(k)}(x_1,\dots,x_k;\widehat{J})\}$ indexed by a label $\widehat{J}$ with distribution $P^{(k)}_{\widehat{J}}$. Each factor $\psi_a(\,\cdot\,)$ is taken equal to $\psi^{(k)}(\cdots;\widehat{J}_a)$ independently with the same distribution. We also introduce explicitly a degree-one factor $\psi_i(x_i)$ connected to each variable node $i\in V$. This are also drawn independently from a list of possible factors $\{\psi(x;J)\}$, indexed by a label J with distribution P_J.

For a random graphical model, the measure $\mu(\,\cdot\,)$ becomes random, and so does its decomposition in extremal Bethe states, in particular the probabilities $\{w_n\}$, and the message sets $\{\nu^n_{i\to a},\widehat{\nu}^n_{a\to i}\}$. In particular, the 1RSB messages $\{Q_{ia},\widehat{Q}_{ai}\}$ become random. It is important to keep in mind the 'two levels' of randomness. Given an edge (ia), the message $\nu^n_{i\to a}$ is random if the Bethe state n is drawn from the distribution w_n. The resulting distribution $Q_{ia}(\mathtt{m})$ becomes a random variable when the graphical model is itself random.

The distributions of $Q_{ia}(\mathtt{m})$, $\widehat{Q}_{ai}(\widehat{\mathtt{m}})$ can then be studied through the density evolution method of Sec. 14.6.2. Let us assume an i.i.d. initialization $Q^{(0)}_{ia}(\,\cdot\,)\stackrel{\rm d}{=}$

$Q^{(0)}(\,\cdot\,)$ (respectively $\widehat{Q}^{(0)}_{ai}(\,\cdot\,) \stackrel{\mathrm{d}}{=} \widehat{Q}^{(0)}(\,\cdot\,)$), and denote by $Q^{(t)}_{ia}(\,\cdot\,)$, $\widehat{Q}^{(t)}_{ai}(\,\cdot\,)$ the 1RSB messages along edge (ia) after t parallel updates using the 1RSB equations (19.28), (19.29). If (ia) is a uniformly random edge then, as $N \to \infty$, $Q^{(t)}_{ia}(\,\cdot\,)$ converges in distribution[29] to $Q^{(t)}(\,\cdot\,)$ (respectively $\widehat{Q}^{(t)}_{ia}(\,\cdot\,)$ converges in distribution to $\widehat{Q}^{(t)}(\,\cdot\,)$). The distributions $Q^{(t)}(\,\cdot\,)$ and $\widehat{Q}^{(t)}(\,\cdot\,)$ are themselves random variables that satisfy the equations:

$$Q^{(t+1)}(\mathtt{m}) \stackrel{\mathrm{d}}{\cong} \sum_{\{\widehat{\mathtt{m}}_b\}} \mathbb{I}\left(\mathtt{m} = \mathsf{f}(\{\widehat{\mathtt{m}}_b\}; J)\right)\; z(\{\widehat{\mathtt{m}}_b\}; J)^{\mathtt{x}} \prod_{b=1}^{l-1} \widehat{Q}^{(t)}_b(\widehat{\mathtt{m}}_b)\,, \tag{19.35}$$

$$\widehat{Q}^{(t)}(\widehat{\mathtt{m}}) \stackrel{\mathrm{d}}{\cong} \sum_{\{\mathtt{m}_j\}} \mathbb{I}\left(\widehat{\mathtt{m}} = \hat{\mathsf{f}}(\{\mathtt{m}_j\}; \widehat{J})\right)\; \hat{z}(\{\mathtt{m}_j\}; \widehat{J})^{\mathtt{x}} \prod_{j=1}^{k-1} Q^{(t)}_j(\mathtt{m}_j)\,, \tag{19.36}$$

where k and l are distributed according to the edge perspective degree profiles ρ_k and λ_l, the $\left\{\widehat{Q}^{(t)}_b\right\}$ are $k-1$ independent copies of $\widehat{Q}^{(t)}(\,\cdot\,)$, and $\left\{Q^{(t)}_j\right\}$ are $l-1$ independent copies of $Q^{(t)}(\,\cdot\,)$. The functions z and $\hat{z}$ are given by:

$$\begin{aligned} z(\{\widehat{\mathtt{m}}_b\}; J) &= \sum_x \psi(x, J) \prod_{b=1}^{l-1} \widehat{\mathtt{m}}_b(x) \\ \hat{z}(\{\mathtt{m}_j\}; \widehat{J}) &= \sum_{x_1,\cdots,x_k} \psi^{(k)}(x_1, \cdots, x_k; \widehat{J}) \prod_{j=1}^{k-1} \mathtt{m}_j(x_j) \end{aligned} \tag{19.37}$$

Within the 1RSB cavity method, the actual distribution of $Q_{i\to a}$ is assumed to coincide with one of the fixed points of the above density evolution equations. As for the RS case, one hopes that, on large enough instances, the message passing algorithm will converge to messages distributed according to this fixed point equation (meaning that there is no problem in exchanging the limits $t \to \infty$ and $N \to \infty$). This can be checked numerically.

For random graphical models, the 1RSB free-entropy density converges to a finite limit $\mathrm{f}^{\mathrm{RSB}}(\mathtt{x})$. This can be expressed in terms of the distributions of Q, $\widehat{Q}$. by taking expectation of Eqs. (19.30) to (19.32), and assuming that 1RSB messages incoming at the same node are i.i.d.. As in (14.77) the result takes the form:

$$\mathrm{f}^{\mathrm{RSB}} = \mathrm{f}^{\mathrm{RSB}}_{\mathrm{v}} + n_{\mathrm{f}} \mathrm{f}^{\mathrm{RSB}}_{\mathrm{f}} - n_{\mathrm{e}} \mathrm{f}^{\mathrm{RSB}}_{\mathrm{e}}\;. \tag{19.38}$$

Here n_{f} is the average number of function nodes per variable (equal to $\Lambda'(1)/P'(1)$ for a graphical model in the $\mathbb{D}_N(\Lambda, P)$ ensemble, and to α for a graphical model in the $\mathbb{G}_N(K, \alpha)$ ensemble) and n_{e} is the number of edges per variable (equal to

[29] We shall not discuss the measure-theoretic subtleties related to this statement. Let us just mention that weak topology is understood on the space of messages $Q^{(t)}$.

$\Lambda'(1)$ and to $K\alpha$ in these two ensembles). The contribution from variable nodes $\mathrm{f}_{\mathrm{v}}^{\mathrm{RSB}}$, function nodes $\mathrm{f}_{\mathrm{f}}^{\mathrm{RSB}}$, and edges $\mathrm{f}_{\mathrm{e}}^{\mathrm{RSB}}$ are:

$$
\begin{aligned}
\mathrm{f}_{\mathrm{v}}^{\mathrm{RSB}} &= \mathbb{E}_{l,J,\{\widehat{Q}\}} \log \left\{ \sum_{\{\widehat{\mathtt{m}}_1,\dots,\widehat{\mathtt{m}}_l\}} \widehat{Q}_1(\widehat{\mathtt{m}}_1)\dots\widehat{Q}_l(\widehat{\mathtt{m}}_l) \left[\sum_{x\in\mathcal{X}} \widehat{\mathtt{m}}_1(x)\dots\widehat{\mathtt{m}}_l(x)\psi(x;J) \right]^{\mathtt{x}} \right\} ,
\\
\mathrm{f}_{\mathrm{f}}^{\mathrm{RSB}} &= \mathbb{E}_{k,\widehat{J},\{Q\}} \log \left\{ \sum_{\{\mathtt{m}_1,\dots,\mathtt{m}_k\}} Q_1(\mathtt{m}_1)\dots Q_k(\mathtt{m}_k) \right.
\\
&\qquad\qquad \left. \left[\sum_{x_1,\dots,x_k\in\mathcal{X}} \mathtt{m}_1(x_1)\dots\mathtt{m}_k(x_k)\psi^{(k)}(x_1,\dots,x_k;\widehat{J}) \right]^{\mathtt{x}} \right\} ,
\\
\mathrm{f}_{\mathrm{e}}^{\mathrm{RSB}} &= \mathbb{E}_{\widehat{Q},Q} \log \left\{ \sum_{\widehat{\mathtt{m}},\mathtt{m}} \widehat{Q}(\widehat{\mathtt{m}})Q(\mathtt{m}) \left[\sum_{x\in\mathcal{X}} \widehat{\mathtt{m}}(x)\mathtt{m}(x) \right]^{\mathtt{x}} \right\} . \qquad (19.39)
\end{aligned}
$$

19.2.6 *Numerical implementation*

Needless to say, it is extremely challenging to find a fixed point of the density evolution equations (19.35), (19.36), and thus determine the distributions of $Q, \widehat{Q}$. A simple numerical approach consists in generalizing the population dynamics algorithm described in the context of the RS cavity method, cf. Sec. 14.6.3.

There are two important issues related to such a generalization:

(*i*) We seek the distribution of $Q(\,\cdot\,)$ (and $\widehat{Q}(\,\cdot\,)$), which is itself a distribution of messages. If we approximate $Q(\,\cdot\,)$ by a sample (a 'population'), we will thus need two level of populations. In other words we will seek a population $\{\mathtt{m}_r^s\}$ with NM items. For each $r \in \{1,\dots,N\}$, the set of messages $\{\mathtt{m}_r^s\},\ s \in \{1,\dots,M\}$ represents a distribution $Q_r(\,\cdot\,)$ (ideally, it would be an i.i.d. sample from this distribution). At the next level, the population $\{Q_r(\,\cdot\,)\}\,,\ r \in \{1,\cdots,N\}$ represents the distribution of $Q(\,\cdot\,)$ (ideally, an i.i.d. sample).

Analogously, for function-to-variable messages, we will use a population $\{\widehat{\mathtt{m}}_r^s\}$, with $r \in \{1,\dots,N\}$ and $s \in \{1,\dots,M\}$.

(*ii*) The re-weighting factors $z(\{\widehat{\mathtt{m}}_b\};J)^{\mathtt{x}}$ and $\hat{z}(\{\mathtt{m}_j\};\widehat{J})^{\mathtt{x}}$ appearing in Eqs. (19.35) and (19.36) do not have any analog in the RS context. How can one take such factors into account when $Q(\,\cdot\,)$, $\widehat{Q}(\,\cdot\,)$ are represented as populations? One possibility is to generate an intermediate weighted population, and than sample from it with a probability proportional to the weight.

This procedure is summarized in the following pseudocode.

1RSB POPULATION DYNAMICS (Model ensemble, Sizes N, M, Iterations T)

Initialize $\{\mathtt{m}_r^s\}$;
for $t = 1, \dots, T$:
  for $r = 1, \dots, N$:
    Draw an integer k with distribution ρ;
    Draw $i(1), \dots, i(k-1)$ uniformly in $\{1, \dots, N\}$;
    Draw $\widehat{J}$ with distribution $P_{\widehat{J}}^{(k)}$;
    for $s = 1, \dots, M$:
      Draw $s(1), \dots, s(k-1)$ uniformly in $\{1, \dots, M\}$;
      Compute $\widehat{\mathtt{m}}_{\mathtt{temp}}^s = \hat{\mathtt{f}}(\mathtt{m}_{i(1)}^{s(1)}, \cdots, \mathtt{m}_{i(k-1)}^{s(k-1)}; \widehat{J})$
      Compute $W^s = \hat{z}(\mathtt{m}_{i(1)}^{s(1)}, \cdots, \mathtt{m}_{i(k-1)}^{s(k-1)}; \widehat{J})^{\mathtt{x}}$
    end;
    Generate the new population
      $\{\widehat{\mathtt{m}}_r^s\}_{s\in[M]} = \text{REWEIGHT}(\{\widehat{\mathtt{m}}_{\mathtt{temp}}^s, W^s\}_{s\in[M]})$
  end;
  for $r = 1, \dots, N$:
    Draw an integer l with distribution λ;
    Draw $i(1), \dots, i(l-1)$ uniformly in $\{1, \dots, N\}$;
    Draw J with distribution P;
    for $s = 1, \dots, M$:
      Draw $s(1), \dots, s(l-1)$ uniformly in $\{1, \dots, M\}$;
      Compute $\mathtt{m}_{\mathtt{temp}}^s = \mathtt{f}(\widehat{\mathtt{m}}_{i(1)}^{s(1)}, \cdots, \widehat{\mathtt{m}}_{i(l-1)}^{s(k-1)}; J)$
      Compute $W^s = z(\widehat{\mathtt{m}}_{i(1)}^{s(1)}, \cdots, \widehat{\mathtt{m}}_{i(l-1)}^{s(l-1)}; J)^{\mathtt{x}}$
    end;
    Generate the new population
      $\{\mathtt{m}_r^s\}_{s\in[M]} = \text{REWEIGHT}(\{\mathtt{m}_{\mathtt{temp}}^s, W^s\}_{s\in[M]})$
end;
return $\{\widehat{\mathtt{m}}_r^s\}$ and $\{\mathtt{m}_r^s\}$.

The re-weighting procedure is given by:

REWEIGHT (Population of messages/weights $\{(\mathtt{m}_{\mathtt{temp}}^s, W^s)\}_{s\in[M]}$)

for $s = 1, \dots, M$, set $p^s \equiv W^s / \sum_{s'} W^{s'}$;
for $s = 1, \dots, M$:
  Draw $i \in \{1, \dots, M\}$ with distribution p^s;
  Set $\mathtt{m}_{\mathtt{new}}^s = \mathtt{m}_{\mathtt{temp}}^i$;
end;
return $\{\mathtt{m}_{\mathtt{new}}^s\}_{s\in[M]}$.

In the large N, M limit, the populations generated by this algorithm should converge to i.i.d. samples distributed as $Q^{(T)}(\,\cdot\,)$, $\widehat{Q}^{(T)}(\,\cdot\,)$, cf. Eq. (19.35), (19.36).

By letting T grow they should represent accurately the fixed points of density evolution, although the caveats expressed in the RS case should be repeated here.

Among the other quantities, the populations generated by this algorithm allow to estimate the 1RSB free-entropy density (19.38). Suppose we have generated a population of messages $\{\widehat{\mathtt{m}}^s_r(\,\cdot\,)\}$, whereby each message is a probability distribution on $\mathcal{X}$. The corresponding estimate of $\mathrm{f}_{\mathrm{v}}^{\mathrm{RSB}}$ is:

$$\widehat{\mathrm{f}}_{\mathrm{v}}^{\mathrm{RSB}} = \mathbb{E}_{l,J}\frac{1}{N^l}\sum_{r(1)\dots r(l)=1}^{N}\log\left\{\frac{1}{M^l}\sum_{s(1),\dots,s(l)=1}^{M}\left[\sum_{x\in\mathcal{X}}\widehat{\mathtt{m}}^{s(1)}_{r(1)}(x)\cdots\widehat{\mathtt{m}}^{s(l)}_{r(l)}(x)\;\psi(x;J)\right]^{\mathtt{x}}\right\}.$$

Similar expressions are easily written for $\mathrm{f}_{\mathrm{f}}^{\mathrm{RSB}}$ and $\mathrm{f}_{\mathrm{e}}^{\mathrm{RSB}}$. Their (approximate) evaluation can be accelerated considerably by summing over a random subset of the l-uples $r(1),\dots,r(l)$ and $s(1),\dots,s(l)$. Further, as in the RS case, it is beneficial to average over iterations (equivalently, over T) in order to reduce statistical errors at small computational cost.

19.3 A first application: XORSAT

Let us apply the 1RSB cavity method to XORSAT. This approach was already introduced in Sec. 18.6, but we want to show how it follows as a special case of the formalism developed in the previous sections. Our objective is to exemplify the general ideas on a well understood problem, and to build basic intuition that will be useful in more complicated applications.

As in Ch. 18 we consider the distribution over $\underline{x} = (x_1,\dots,x_N) \in \{\mathtt{0},\mathtt{1}\}^N$ specified by

$$\mu(\underline{x}) = \frac{1}{Z}\prod_{a=1}^{M}\mathbb{I}\left(x_{i_1(a)}\oplus\cdots\oplus x_{i_k(a)} = b_a\right). \tag{19.40}$$

As usual $\oplus$ denotes sum modulo 2 and, for each $a\in\{1,\cdots,M\}$, $\partial a = \{i_1(a),\dots,i_K(a)\}$ is a subset of $\{1,\cdot,N\}$, and $b_a\in\{\mathtt{0},\mathtt{1}\}$. Random K-XORSAT formulae are generated by choosing both the index set $\{i_1(a),\dots,i_K(a)\}$ and the right hand side b_a uniformly at random.

19.3.1 *BP equations*

The BP equations read:

$$\mathtt{m}_{ia}(x_i) = \frac{1}{z_{ia}}\prod_{b\in\partial i\setminus a}\widehat{\mathtt{m}}_{bi}(x_i)\,, \tag{19.41}$$

$$\widehat{\mathtt{m}}_{ai}(x_i) = \frac{1}{\hat{z}_{ai}}\sum_{\underline{x}_{\partial a\setminus i}}\mathbb{I}\left(x_{i_1(a)}\oplus\cdots\oplus x_{i_K(a)} = b_a\right)\prod_{j\in\partial a\setminus i}\mathtt{m}_{ja}(x_j)\,. \tag{19.42}$$

As in Sec. 18.6, we shall assume that messages can take only three values, which we denote by the shorthands: $\mathtt{m}_{ia} = \mathtt{0}$ if $(\mathtt{m}_{ia}(\mathtt{0}) = 1,\ \mathtt{m}_{ia}(\mathtt{1}) = 0)$; $\mathtt{m}_{ia} = \mathtt{1}$ if $(\mathtt{m}_{ia}(\mathtt{0}) = 0,\ \mathtt{m}_{ia}(\mathtt{1}) = 1)$; $\mathtt{m}_{ia} = *$ if $(\mathtt{m}_{ia}(\mathtt{0}) = \mathtt{m}_{ia}(\mathtt{1}) = 1/2)$.

Consider the first BP equation (19.41), and denote by n_0, n_1, n_* the number of messages of type 0, 1, $*$ in the set of incoming messages $\{\widehat{\mathtt{m}}_{bi}\}$, $b \in \partial i \backslash a$. Then Eq. (19.41) can be rewritten as:

$$\mathtt{m}_{ia} = \begin{cases} \mathtt{0} & \text{if } n_0 > 0,\, n_1 = 0, \\ \mathtt{1} & \text{if } n_0 = 0,\, n_1 > 0, \\ * & \text{if } n_0 = 0,\, n_1 = 0, \\ ? & \text{if } n_0 > 0,\, n_1 > 0, \end{cases} \qquad z_{ia} = \begin{cases} 2^{-n_*} & \text{if } n_0 > 0,\, n_1 = 0, \\ 2^{-n_*} & \text{if } n_0 = 0,\, n_1 > 0, \\ 2^{1-n_*} & \text{if } n_0 = 0,\, n_1 = 0, \\ 0 & \text{if } n_0 > 0,\, n_1 > 0. \end{cases} \tag{19.43}$$

The computation of the normalization constant z_{ia} will be useful in the 1RSB analysis. Notice that, if $n_0 > 0$ and $n_1 > 0$, a contradiction arises at node i and therefore $\mathtt{m}_{ia}$ is not defined. However we will see that, because in this case $z_{ia} = 0$, this situation does not create any problem within 1RSB.

In the second BP equation (19.42) denote by $\widehat{n}_0$ (respectively, $\widehat{n}_1$, $\widehat{n}_*$) the number of messages of type 0 (resp. 1, $*$) among $\{\mathtt{m}_{ja}\}$, $j \in \partial a \backslash i$. Then we get

$$\widehat{\mathtt{m}}_{ai} = \begin{cases} \mathtt{0} & \text{if } n_* = 0, \text{ and } n_1 \text{ has the same parity as } b_a, \\ \mathtt{1} & \text{if } n_* = 0, \text{ and } n_1 \text{ has not the same parity as } b_a, \\ * & \text{if } n_* > 0. \end{cases} \tag{19.44}$$

In all three cases $\hat{z}_{ai} = 1$.

In Sec. 18.6 we studied the equations (19.41), (19.42) above and deduced that, for typical random instances with $\alpha = M/N < \alpha_{\rm d}(K)$, they have a unique solution, with $\mathtt{m}_{ia} = \widehat{\mathtt{m}}_{ai} = *$ on each edge.

Exercise 19.2 Evaluate the Bethe free-entropy on this solution, and show that it yields the free-entropy density $\mathrm{f}^{\rm RS} = (1-\alpha)\log 2$.

19.3.2 *The 1RSB cavity equations*

We now assume that the BP equations (19.43), (19.44) have many solutions, and apply the 1RSB cavity method to study their statistics.

The 1RSB messages Q_{ia}, $\widehat{Q}_{ai}$ are distributions over $\{\mathtt{0},\mathtt{1},*\}$. A little effort shows that Eq. (19.28) yields

$$Q_{ia}(\mathtt{0}) = \frac{1}{Z_{ia}} \left\{ \prod_{b\in\partial i\backslash a} \left(\widehat{Q}_{bi}(\mathtt{0}) + 2^{-\mathtt{x}} \widehat{Q}_{bi}(*) \right) - \prod_{b\in\partial i\backslash a} \left(2^{-\mathtt{x}} \widehat{Q}_{bi}(*) \right) \right\}, \tag{19.45}$$

$$Q_{ia}(\mathtt{1}) = \frac{1}{Z_{ia}} \left\{ \prod_{b\in\partial i\backslash a} \left(\widehat{Q}_{bi}(\mathtt{1}) + 2^{-\mathtt{x}} \widehat{Q}_{bi}(*) \right) - \prod_{b\in\partial i\backslash a} \left(2^{-\mathtt{x}} \widehat{Q}_{bi}(*) \right) \right\}, \tag{19.46}$$

$$Q_{ia}(*) = \frac{1}{Z_{ia}} 2^{\mathtt{x}} \prod_{b\in\partial i\backslash a} 2^{-\mathtt{x}} \widehat{Q}_{bi}(*)\,. \tag{19.47}$$

For instance, Eq. (19.45) follows from the first line of Eq. (19.43): $\mathtt{m}_{ia} = \mathtt{0}$ if all the incoming messages are $\widehat{\mathtt{m}}_{bi} \in \{*, \mathtt{0}\}$ (first term), unless they are all equal

to $*$ (subtracted term). The re-weighting $z_{ia}^{\mathtt{x}} = 2^{-\mathtt{x}n_*}$ decomposes into factors associated to the incoming $*$ messages.

The second group of 1RSB equations, Eq. (19.29), takes the form:

$$\widehat{Q}_{ai}(\mathtt{0}) = \frac{1}{2}\left\{\prod_{j\in\partial a\setminus i}(Q_{ja}(\mathtt{0})+Q_{ja}(\mathtt{1})) + s(b_a)\prod_{j\in\partial a\setminus i}(Q_{ja}(\mathtt{0})-Q_{ja}(\mathtt{1}))\right\}, \tag{19.48}$$

$$\widehat{Q}_{ai}(\mathtt{1}) = \frac{1}{2}\left\{\prod_{j\in\partial a\setminus i}(Q_{ja}(\mathtt{0})+Q_{ja}(\mathtt{1})) - s(b_a)\prod_{j\in\partial a\setminus i}(Q_{ja}(\mathtt{0})-Q_{ja}(\mathtt{1}))\right\}, \tag{19.49}$$

$$\widehat{Q}_{ai}(*) = 1 - \prod_{j\in\partial a\setminus i}(Q_{ja}(\mathtt{0})+Q_{ja}(\mathtt{1}))\,, \tag{19.50}$$

where $s(b_a) = +1$ if $b_a = \mathtt{0}$, and $s(b_a) = -1$ otherwise.

Notice that, if one takes $\mathtt{x} = 0$, the two sets of equations coincide with those obtained in Sec. 18.6, see Eq. (18.35) (the homogeneous linear system, $b_a = \mathtt{0}$, was considered there). As in that section, we look for solutions such that the messages $Q_{ia}(\,\cdot\,)$ (respectively $\widehat{Q}_{ai}(\,\cdot\,)$) take two possible values: either $Q_{ia}(\mathtt{0}) = Q_{ia}(\mathtt{1}) = 1/2$, or $Q_{ia}(*) = 1$. This assumption is consistent with the 1RSB cavity equations (19.45) and (19.50). Under this assumption, the $\mathtt{x}$ dependency drops from these equations and we recover the analysis in Sec. 18.6. In particular, we can repeat the density evolution analysis discussed there. If we denote by Q_* the probability that a randomly chosen edge carries the 1RSB message $Q_{ia}(\mathtt{0}) = Q_{ia}(\mathtt{1}) = 1/2$, then the fixed point equation of density evolution reads:

$$Q_* = 1 - \exp\{-k\alpha Q_*^{k-1}\}\,. \tag{19.51}$$

For $\alpha < \alpha_{\rm d}(K)$ this equation admits the only solution $Q_* = 0$, implying $Q_{ia}(*) = 1$ with high probability. This indicates (once more) that the only solution of the BP equations in this regime is $\mathtt{m}_{ia} = *$ for all $(i,a) \in E$.

For $\alpha > \alpha_{\rm d}$ a couple of non-trivial solutions (with $Q_* > 0$) appear, indicating the existence of a large number of BP fixed points (and hence, Bethe measures). Stability under density evolution suggest to select the largest one. It will also be useful in the following to introduce the probability

$$\widehat{Q}_* = Q_*^{k-1} \tag{19.52}$$

that a uniformly random edge carries a message $\widehat{Q}_{ai}(\mathtt{0}) = \widehat{Q}_{ai}(\mathtt{1}) = 1/2$.

19.3.3 *Complexity*

We can now compute the Bethe free-entropy (19.33) of the auxiliary graphical model. The complexity will be computed through the Legendre transform of the 1RSB free-entropy, see Eq. (19.8).

Let us start by computing the contribution $\mathbb{F}_a^{\mathrm{RSB}}$ defined in Eq. (19.30). Consider the weight

$$e^{\mathbb{F}_a(\{\mathtt{m}_{ia}\})} = \sum_{\underline{x}_{\partial a}} \mathbb{I}(x_{i_1(a)} \oplus \cdots \oplus x_{i_K(a)} = b_a) \prod_{i \in \partial a} \mathtt{m}_{ia}(x_i)\,. \tag{19.53}$$

Let $\widehat{n}_{\mathtt{0}}$ (respectively, $\widehat{n}_{\mathtt{1}}$, $\widehat{n}_*$) denote the number of variable nodes $i \in \partial a$ such that $\mathtt{m}_{ia} = \mathtt{0}$ (resp. $\mathtt{1}$, $*$) for $i \in \partial a$. Then we get

$$e^{\mathbb{F}_a(\{\mathtt{m}_{ia}\})} = \begin{cases} 1/2 & \text{if } \widehat{n}_* > 0, \\ 1 & \text{if } \widehat{n}_* = 0 \text{ and } \widehat{n}_{\mathtt{1}} \text{ has the same parity as } b_a, \\ 0 & \text{if } \widehat{n}_* = 0 \text{ and } \widehat{n}_{\mathtt{1}} \text{ has not the same parity as } b_a, \end{cases} \tag{19.54}$$

Taking the expectation of $e^{\mathtt{x}\mathbb{F}_a(\{\mathtt{m}_{ia}\})}$ with respect to $\{\mathtt{m}_{ia}\}$ distributed independently according to $Q_{ia}(\,\cdot\,)$, and assuming $Q_{ia}(\mathtt{0}) = Q_{ia}(\mathtt{1})$ (which is the case in our solution), we get

$$\mathbb{F}_a^{\mathrm{RSB}} = \log\left\{\frac{1}{2}\prod_{i\in\partial a}(1 - Q_{ia}(*)) + \frac{1}{2^{\mathtt{x}}}\left[1 - \prod_{i\in\partial a}(1 - Q_{ia}(*))\right]\right\}. \tag{19.55}$$

The first term corresponds to the case $\widehat{n}_* = 0$ (the factor $1/2$ being the probability that the parity of $\widehat{n}_{\mathtt{1}}$ is b_a), and the second to $\widehat{n}_* > 0$. Within our solution either $Q_{ia}(*) = 0$ or $Q_{ia}(*) = 1$. Therefore only one of the above terms survives: either $Q_{ia}(*) = 0$ for all $i \in \partial a$, yielding $\mathbb{F}_a^{\mathrm{RSB}} = -\log 2$, or $Q_{ia}(*) = 1$ for some $i \in \partial a$, implying $\mathbb{F}_a^{\mathrm{RSB}} = -\mathtt{x}\log 2$.

Until now we considered a generic K-XORSAT instance. For random instances, we can take the expectation with respect to $Q_{ia}(*)$ independently distributed as in the density evolution fixed point. The first case, namely $Q_{ia}(*) = 0$ for all $i \in \partial a$ (and thus $\mathbb{F}_a^{\mathrm{RSB}} = -\log 2$), occurs with probability Q_*^k. The second, i.e. $Q_{ia}(*) = 1$ for some $i \in \partial a$ (and $\mathbb{F}_a^{\mathrm{RSB}} = -\mathtt{x}\log 2$), occurs with probability $1 - Q_*^k$. Altogether we obtain:

$$\mathbb{E}\{\mathbb{F}_a^{\mathrm{RSB}}\} = -\left[Q_*^k + \mathtt{x}(1 - Q_*^k)\right]\log 2 + o_N(1)\,. \tag{19.56}$$

Assuming the messages $Q_{ia}(\,\cdot\,)$ to be short-range correlated, $\sum_{a\in F}\mathbb{F}_a^{\mathrm{RSB}}$ will concentrate around its expectation. We then have, with high probability,

$$\frac{1}{N}\sum_{a\in F}\mathbb{F}_a^{\mathrm{RSB}} = -\alpha\left[Q_*^k + x(1 - Q_*^k)\right]\log 2 + o_N(1)\,. \tag{19.57}$$

The contributions from variable node and edge terms can be computed along similar lines. We will just sketch these computations, and invite the reader to work out the details.

Consider the contribution $\mathbb{F}_i^{\mathrm{RSB}}$, $i \in V$, defined in (19.31). Assume that $\widehat{Q}_{ai}(*) = 1$ (respectively, $\widehat{Q}_{ai}(\mathtt{0}) = \widehat{Q}_{ai}(\mathtt{1}) = 1/2$) for n_* (resp. $n_{\mathtt{0}}$) of the neighboring function nodes $a \in \partial i$. Then $\mathbb{F}_i^{\mathrm{RSB}} = -(n_*\mathtt{x} + n_{\mathtt{0}} - 1)\log 2$ if $n_{\mathtt{0}} \geq 1$, and

$\mathbb{F}_i^{\rm RSB} = -(n_*-1)\mathtt{x}\log 2$ otherwise. Averaging these expressions over $n_{\mathtt{0}}$ (a Poisson distributed random variable with mean $k\alpha\widehat{Q}_*$) and n_* (Poisson with mean $k\alpha(1-\widehat{Q}_*)$) we obtain:

$$\frac{1}{N}\sum_{i\in V}\mathbb{F}_i^{\rm RSB} = -\left\{\left[k\alpha\widehat{Q}_* - 1 + e^{-k\alpha\widehat{Q}_*}\right] + \left[k\alpha(1-\widehat{Q}_*) - e^{-k\alpha\widehat{Q}_*}\right]\mathtt{x}\right\}\log 2 + o_N(1)\,. \tag{19.58}$$

Let us finally consider the edge contribution $\mathbb{F}_{(ia)}^{\rm RSB}$ defined in (19.32). If $Q_{ia}(\mathtt{0}) = Q_{ia}(\mathtt{1}) = 1/2$ and $\widehat{Q}_{ai}(\mathtt{0}) = \widehat{Q}_{ai}(\mathtt{1}) = 1/2$, then either $e^{\mathbb{F}_{ai}} = 1$ or $e^{\mathbb{F}_{ia}} = 0$, each with probability $1/2$. As a consequence $\mathbb{F}_{(ia)}^{\rm RSB} = -\log 2$. If either $Q_{ia}(*) = 1$ or $\widehat{Q}_{ai}(*) = 1$ (or both), $e^{\mathbb{F}_{ia}^{\rm RSB}} = 1/2$ with probability 1, and therefore $\mathbb{F}_{(ia)}^{\rm RSB} = -\mathtt{x}\log 2$. Altogether we obtain, with high probability

$$\frac{1}{N}\sum_{(ia)\in E}\mathbb{F}_{(ia)}^{\rm RSB} = -k\alpha\left\{Q_*\widehat{Q}_* + (1-Q_*\widehat{Q}_*)\mathtt{x}\right\}\log 2 + o_N(1). \tag{19.59}$$

The free-entropy (19.33) of the auxiliary graphical model is obtained by collecting the various terms. We obtain $\mathbb{F}^{\rm RSB}(\mathtt{x}) = N\mathrm{f}^{\rm RSB}(\mathtt{x}) + o(N)$ where $\mathrm{f}^{\rm RSB}(\mathtt{x}) = [\Sigma_{\rm tot} + \mathtt{x}\,\phi_{\rm typ}]\log 2$ and

$$\Sigma_{\rm tot} = k\alpha Q_*\widehat{Q}_* - k\alpha\widehat{Q}_* - \alpha Q_*^k + 1 - e^{-k\alpha\widehat{Q}_*}\,, \tag{19.60}$$

$$\phi_{\rm typ} = -k\alpha Q_*\widehat{Q}_* + k\alpha\widehat{Q}_* + \alpha Q_*^k - \alpha + e^{-k\alpha\widehat{Q}_*}\,. \tag{19.61}$$

Here Q_* is the largest solution of Eq. (19.51) and $\widehat{Q}_* = Q_*^{k-1}$, a condition that has a pleasing interpretation as shown in the exercise below.

Exercise 19.3 Consider the function $\Sigma_{\rm tot}(Q_*, \widehat{Q}_*)$ defined in Eq. (19.60). Show that the stationary points of this function coincide with the solutions of Eq. (19.51) and $\widehat{Q}_* = Q_*^{k-1}$.

Because of the linear dependence on x, the Legendre transform (19.8) is straightforward

$$\Sigma(\phi) = \begin{cases} \Sigma_{\rm tot} & \text{if } \phi = \phi_{\rm typ}, \\ -\infty & \text{otherwise.} \end{cases} \tag{19.62}$$

This means that there are $2^{N\Sigma_{\rm tot}}$ Bethe measures which all have the same entropy $N\phi_{\rm typ}\log 2$. Furthermore, $\Sigma_{\rm tot} + \phi_{\rm typ} = 1-\alpha$, confirming that the total entropy is $(1-\alpha)\log 2$. This identity can be also written in the form

$$\frac{1}{2^{N(1-\alpha)}} = \frac{1}{2^{N\Sigma_{\rm tot}}} \times \frac{1}{2^{N\phi_{\rm typ}}}\,, \tag{19.63}$$

which is nothing but the decomposition (19.6) in extremal Bethe measures. Indeed, if $\underline{x}$ is a solution of the linear system, $\mu(\underline{x}) = 1/2^{N(1-\alpha)}$, $w_n \approx 1/2^{N\Sigma_{\rm tot}}$,

and (assuming the μ^n to have disjoint supports) $\mu^n(\underline{x}) \approx 1/2^{N\phi_{\rm typ}}$ for the state n which contains $\underline{x}$.

Note that the value of Σ that we find here coincides with the result that we obtained in Sec. 18.5 for the logarithm of the number of clusters in random XORSAT formulae. This provides an independent check of our assumptions, and in particular it shows that the number of clusters is, to leading order, the same as the number of Bethe measures. In particular, the SAT-UNSAT transition occurs at the value of α where the complexity $\Sigma_{\rm tot}$ vanishes. At this value each cluster still contains a large number, $2^{N(1-\alpha_s)}$, of configurations.

Exercise 19.4 Repeat this 1RSB cavity analysis for a linear Boolean system described by a factor graph from the ensemble $\mathbb{D}_N(\Lambda, P)$ (This means a random system of linear equations, whereby the fraction of equations involving k variables is P_k, and the fraction of variables which appear in exactly ℓ equations is Λ_ℓ):

(*a*) Show that Q_* and $\widehat{Q}_*$ satisfy:

$$\widehat{Q}_* = \rho(Q_*) \quad ; \quad Q_* = 1 - \lambda(1 - \widehat{Q}_*) \ , \tag{19.64}$$

where λ and ρ are the edge perspective degree profiles.

(*b*) Show that the complexity is given by

$$\Sigma_{\rm tot} = 1 - \frac{\Lambda'(1)}{P'(1)}\, P(Q_*) - \Lambda(1 - \widehat{Q}_*) - \Lambda'(1)(1 - Q_*)\widehat{Q}_* \tag{19.65}$$

and the internal entropy of the clusters is $\phi_{\rm typ} = 1 - \Lambda'(1)/P'(1) - \Sigma_{\rm tot}$.

(*c*) In the case where all variables have degree strictly larger than 1 (so that $\lambda(0) = 0$), argue that the relevant solution is $Q_* = \widehat{Q}_* = 1$, $\Sigma_{\rm tot} = 1 - \Lambda'(1)/P'(1)$, $\phi_{\rm typ} = 0$. What is the interpretation of this result in terms of the core structure discussed in Sec. 18.3?

19.4 The special value $\mathtt{x} = 1$

Let us return to the general formalism. The $\mathtt{x} = 1$ case plays a special role, in that the weights $\{w_n(\mathtt{x})\}$ of various Bethe measures in the auxiliary model, coincide with the ones appearing in the decomposition (19.6). This fact manifests itself in some remarkable properties of the 1RSB formalism.

19.4.1 *Back to BP*

Consider the general 1RSB cavity equations (19.28), (19.29). Using the explicit form of the re-weighting factors $e^{\mathbb{F}_i - \mathbb{F}_{ia}}$ and $e^{\mathbb{F}_a - \mathbb{F}_{ia}}$ provided in Eqs. (19.23), (19.24), they can be written, for $\mathtt{x} = 1$, as:

$$Q_{ia}(\mathtt{m}_{ia}) \cong \sum_{x_i} \sum_{\{\widehat{\mathtt{m}}_{bi}\}} \mathbb{I}\left(\mathtt{m}_{ia} = g_i(\{\widehat{\mathtt{m}}_{bi}\})\right) \prod_{b\in\partial i\setminus a} \widehat{Q}_{bi}(\widehat{\mathtt{m}}_{bi})\, \widehat{\mathtt{m}}_{bi}(x_i)\,, \tag{19.66}$$

$$\widehat{Q}_{ai}(\widehat{\mathtt{m}}_{ai}) \cong \sum_{\underline{x}_{\partial a}} \psi_a(\underline{x}_{\partial a}) \sum_{\{\mathtt{m}_{ja}\}} \mathbb{I}\left(\widehat{\mathtt{m}}_{ai} = f_a(\{\mathtt{m}_{ja}\})\right) \prod_{j\in\partial a\setminus i} Q_{ja}(\mathtt{m}_{ja})\, \mathtt{m}_{ja}(x_j)\,. \tag{19.67}$$

Let us introduce the messages obtained by taking the averages of the 1RSB ones $\{Q_{ia}, \widehat{Q}_{ai}\}$:

$$\nu^{\rm av}_{i\to a}(x_i) \equiv \sum_{\mathtt{m}_{ia}} Q_{ia}(\mathtt{m}_{ia})\, \mathtt{m}_{ia}(x_i)\,, \quad \widehat{\nu}^{\rm av}_{a\to i}(x_i) \equiv \sum_{\widehat{\mathtt{m}}_{ai}} \widehat{Q}_{ai}(\widehat{\mathtt{m}}_{ai})\, \widehat{\mathtt{m}}_{ai}(x_i)\,.$$

The interpretation of these quantities is straightforward. Given an extremal Bethe measure sampled according to the distribution w_n, let $\nu^n_{i\to a}(\,\cdot\,)$ (respectively $\widehat{\nu}^n_{a\to i}(\,\cdot\,)$) be the corresponding message along the directed edge $i\to a$ (resp. $a\to i$). Its expectation, with respect to the random choice of the measure, is $\nu^{\rm av}_{i\to a}(\,\cdot\,)$ (respectively $\widehat{\nu}^{\rm av}_{a\to i}(\,\cdot\,)$).

Using the expressions (19.9), one finds that Eqs. (19.66), (19.67) imply

$$\nu^{\rm av}_{i\to a}(x_i) \cong \prod_{b\in\partial i\setminus a} \widehat{\nu}^{\rm av}_{b\to i}(x_i)\,, \tag{19.68}$$

$$\widehat{\nu}^{\rm av}_{a\to i}(x_i) \cong \sum_{\{x_j\}_{j\in\partial a\setminus i}} \psi_a(\underline{x}_{\partial a}) \prod_{j\in\partial a\setminus i} \nu^{\rm av}_{j\to a}(x_j)\,, \tag{19.69}$$

which are nothing but the ordinary BP equations. This suggests that, even if $\mu(\,\cdot\,)$ decomposes into an exponential number of extremal Bethe measures $\mu^n(\,\cdot\,)$, it is itself a (non-extremal) Bethe measure. In particular, there exists a quasi-solution of BP equations associated with it, that allows to compute its marginals.

The reader might be disappointed by these remarks. Why insisting on the 1RSB cavity approach if, when the 'correct' weights are used, one recovers the much simpler BP equations? There are at least two answers:

1. The 1RSB approach provides a much more refined picture: decomposition in extremal Bethe states, long range correlations, complexity. This is useful and interesting *per se*.
2. In the cases of a static (s1RSB) phase, it turns out that the region $\mathtt{x} = 1$ corresponds to an 'unphysical' solution of the 1RSB cavity equations, and that (asymptotically) correct marginals are instead obtained by letting $\mathtt{x} = \mathtt{x}_*$, for some $\mathtt{x}_* \in [0, 1)$. In such cases it is mandatory to resort to the full 1RSB formalism (see Sec. 19.6 below).

19.4.2 *A simpler recursion*

As we stressed above, controlling (either numerically or analytically) the 1RSB distributional recursions (19.35), (19.36) is a difficult task. In the case $\mathtt{x} = 1$, they simplify considerably and lend themselves to a much more accurate numerical study. This remark can be very useful in practice.

As in Sec. 19.2.5, we consider a random graphical model. We shall also assume a 'local uniformity condition.' More precisely, the original model $\mu(\,\cdot\,)$ is a Bethe measure for the message set $\nu^{\rm av}_{i\to a}(x_i) = 1/q$ and $\widehat{\nu}^{\rm av}_{a\to i}(x_i) = 1/q$, where $q = |\mathcal{X}|$ is the size of the alphabet. While such a local uniformity condition is not necessary, it considerably simplify the derivation below. The reader can find a more general treatment in the literature.

Consider Eqs. (19.35) and (19.36) at $\mathtt{x} = 1$. The normalization constants can be easily computed using the uniformity condition. We can then average over the structure of the graph, and the function node distribution: let us denote by $Q_{\rm av}$ and $\widehat{Q}_{\rm av}$ the averaged distributions. They satisfy the following equations:

$$Q^{(t+1)}_{\rm av}(\mathtt{m}) = \mathbb{E}\left\{ q^{l-2} \sum_{\{\widehat{\mathtt{m}}_b\}} \mathbb{I}\left(\mathtt{m} = \mathtt{f}(\{\widehat{\mathtt{m}}_b\}; J)\right)\; z(\{\widehat{\mathtt{m}}_b\}) \prod_{b=1}^{l-1} \widehat{Q}^{(t)}_{\rm av}(\widehat{\mathtt{m}}_b) \right\}\,, \tag{19.70}$$

$$\widehat{Q}^{(t)}_{\rm av}(\widehat{\mathtt{m}}) = \mathbb{E}\left\{ \frac{q^{k-2}}{\overline{\psi}_k} \sum_{\{\mathtt{m}_j\}} \mathbb{I}\left(\widehat{\mathtt{m}} = \hat{\mathtt{f}}(\{\mathtt{m}_j\}; \widehat{J})\right)\; \hat{z}(\{\mathtt{m}_j\}; \widehat{J}) \prod_{j=1}^{k-1} Q^{(t)}_{\rm av}(\mathtt{m}_j) \right\}\,, \tag{19.71}$$

where expectations are taken over $l, k, J, \widehat{J}$, distributed according to the random graphical model. Here $\overline{\psi}_k = \sum_{x_1,\dots,x_{k-1}} \psi(x_1,\dots,x_{k-1},x;\widehat{J})$ can be shown to be independent of x (this is necessary for the uniformity condition to hold).

Equations (19.70) and (19.71) are considerably simpler that the original distributional equations (19.35), (19.36) in that $Q^{(t)}_{\rm av}(\,\cdot\,)$, $\widehat{Q}^{(t)}_{\rm av}(\,\cdot\,)$ are non-random. On the other hand, they still involve a reweighting factor that is difficult to handle. It turns out that this reweighting can be eliminated by introducing a new couple of distributions for each $x \in \mathcal{X}$:

$$\widehat{R}^{(t)}_x(m) \equiv q\, m(x)\, \widehat{Q}^{(t)}_{\rm av}(m)\,, \qquad R^{(t)}_x(m) = q\, m(x)\, Q^{(t)}_{\rm av}(m)\,. \tag{19.72}$$

One can show that Eqs. (19.70), (19.71) imply the following recursions for $R^{(t)}_x$, $\widehat{R}^{(t)}_x$,

$$R^{(t+1)}_x(\mathtt{m}) = \mathbb{E}\left\{ \sum_{\{\widehat{\mathtt{m}}_b\}} \mathbb{I}\left(\mathtt{m} = g(\{\widehat{\mathtt{m}}_b\}; J)\right) \prod_{b=1}^{l-1} \widehat{R}^{(t)}_x(\widehat{\mathtt{m}}_b) \right\}\,, \tag{19.73}$$

$$\widehat{R}^{(t)}_x(\widehat{\mathtt{m}}) = \mathbb{E}\left\{ \sum_{\{x_j\}} \pi(\{x_j\}|x;\widehat{J}) \sum_{\{\mathtt{m}_j\}} \mathbb{I}\left(\widehat{\mathtt{m}} = f(\{\mathtt{m}_j\}; \widehat{J})\right) \prod_{j=1}^{k-1} R^{(t)}_{x_j}(\mathtt{m}_j) \right\} \tag{19.74}$$

Here $\mathbb{E}$ denotes expectation with respect to $l, \widehat{J}, k, J$ and, for any x, $\widehat{J}$, the distribution $\pi(\{x_j\}|x;\widehat{J})$ is defined by

$$\pi(x_1,\dots,x_{k-1}|x;\widehat{J}) = \frac{\psi(x_1,\dots,x_{k-1},x;\widehat{J})}{\sum_{y_1,\dots,y_{k-1}} \psi(y_1,\dots,y_{k-1},x;\widehat{J})}\,. \tag{19.75}$$

Exercise 19.5 Prove formulas (19.73) and (19.74). It might be useful to recall the following explicit expressions for the reweighting factors z and $\hat{z}$:

$$z(\{\widehat{\mathtt{m}}_b\})\,\mathtt{m}(x) = \prod_{b=1}^{l-1} \widehat{\mathtt{m}}_b(x)\,, \tag{19.76}$$

$$\hat{z}(\{\mathtt{m}_j\};\widehat{J})\,\widehat{\mathtt{m}}(x) = \sum_{\{x_i\},x} \psi(x_1,\dots,x_{k-1},x;\widehat{J}) \prod_{j=1}^{k-1} \mathtt{m}_j(x_j)\,. \tag{19.77}$$

The equations (19.73), (19.74) have a simple operational description. Let $\widehat{J}$ and k be drawn according to their distribution, and, given x, generate $x_1,\dots,x_{k-1}$ according to the kernel $\pi(x_1,\dots,x_k|x;\widehat{J})$. Then draw independent messages $\mathtt{m}_1,\dots,\mathtt{m}_{k-1}$ with distribution (respectively) $R^{(t)}_{x_1},\dots,R^{(t)}_{x_{k-1}}$. According to Eq. (19.74), $\widehat{\mathtt{m}} = f(\{\mathtt{m}_j\};\widehat{J})$ has then distribution $\widehat{R}^{(t)}_x$. For Eq. (19.73), draw J and l according to their distribution. Given x, draw $l-1$ i.i.d. messages $\widehat{\mathtt{m}}_1,\dots,\widehat{\mathtt{m}}_{l-1}$ with distribution $\widehat{R}^{(t)}_x$. Them $\mathtt{m} = g(\{\widehat{\mathtt{m}}_b\};J)$ has distribution $R^{(t+1)}_x$.

We will see in Ch. 22 that this procedure does indeed coincide with the one for computing 'point-to-set correlations' with respect to the measure $\mu(\,\cdot\,)$.

To summarize, for $\mathtt{x}=1$ we have succeeded in simplifying the 1RSB density evolution equations in two directions: (*i*) The resulting equations do not involve 'distributions of distributions;' (*ii*) We got rid of the reweighting factor. A third crucial simplification is the following:

Theorem 19.5 *The 1RSB equations have a non trivial solution (meaning a solution different from the RS one) if and only if Eqs. (19.73), (19.74), when initialized with $R^{(0)}_x$ being a singleton distribution on $\mathtt{m}(y) = \mathbb{I}(y=x)$, converge as $t\to\infty$, to a non-trivial distribution.*

This theorem resolves (in the case $\mathtt{x}=1$) the ambiguity on the initial condition of the 1RSB iteration. In other words, if the 1RSB equations admit a non-trivial solution, it can be reached if we iterate the equations starting from the initial condition mentioned in the theorem. We refer the reader to the literature for the proof.

Exercise 19.6 Show that the free-entropy of the auxiliary model $\mathbb{F}^{\rm RSB}(\mathtt{x})$, evaluated at $\mathtt{x}=1$, coincides with the RS Bethe free-entropy.

Further, its derivative with respect to $\mathtt{x}$ at $\mathtt{x}=1$ can be expressed in terms of the fixed point distributions $R^{(\infty)}_x$ and $\widehat{R}^{(\infty)}_x$. In particular the complexity and internal free-entropy can be computed from the fixed points of the simplified equations (19.73), (19.74).

The conclusion of this section is that 1RSB calculations at $\mathtt{x}=1$ are not technically harder that RS ones. In view of the special role played by the value

$\mathtt{x} = 1$ this observation can be exploited in a number of contexts.

19.5 Survey propagation

The 1RSB cavity method can be applied to other message passing algorithms whenever these have many fixed points. A particularly important case is the min-sum algorithm of Sec. 14.3. This approach (both in its RS and 1RSB versions) is sometimes referred to as the **energetic cavity method** because, in physics terms, the min-sum algorithm aims at computing the ground state configuration and its energy. We will call the corresponding 1RSB message passing algorithm $\mathsf{SP}(\mathtt{y})$ (survey propagation at finite $\mathtt{y}$).

19.5.1 *The* $\mathsf{SP}(\mathtt{y})$ *equations*

The formalism follows closely the one used with BP solutions. To emphasize the similarities, let us adopt the same notation for the min-sum messages as for the BP ones. We define

$$\mathtt{m}_{ja}(x_j) \equiv E_{i\to a}(x_i)\,, \quad \widehat{\mathtt{m}}_{ai}(x_i) \equiv \widehat{E}_{a\to i}(x_i)\,, \tag{19.78}$$

and write the min-sum equations (14.40), (14.41) as:

$$\mathtt{m}_{ia} = \mathsf{f}^{\mathrm{e}}_i\left(\{\widehat{\mathtt{m}}_{bi}\}_{b\in\partial i\setminus a}\right)\,, \qquad \widehat{\mathtt{m}}_{ai} = \hat{\mathsf{f}}^{\mathrm{e}}_a\left(\{\mathtt{m}_{ja}\}_{j\in\partial a\setminus i}\right)\,. \tag{19.79}$$

The functions $\mathsf{f}^{\mathrm{e}}_i$, $\hat{\mathsf{f}}^{\mathrm{e}}_a$ are defined by Eqs. (14.40), (14.41), that we reproduce here:

$$\mathtt{m}_{ia}(x_i) = \sum_{b\in\partial i\setminus a} \widehat{\mathtt{m}}_{bi}(x_i) - u_{ia}\,, \tag{19.80}$$

$$\widehat{\mathtt{m}}_{ai}(x_i) = \min_{\underline{x}_{\partial a\setminus i}}\left[E_a(\underline{x}_{\partial a}) + \sum_{j\in\partial a\setminus i}\mathtt{m}_{ja}(x_j)\right] - \hat{u}_{ai}\,, \tag{19.81}$$

where $u_{ia}, \hat{u}_{ai}$ are normalization constants (independent of x_i) which ensure that $\min_{x_i}\widehat{\mathtt{m}}_{ai}(x_i) = 0$ and $\min_{x_i}\mathtt{m}_{ia}(x_i) = 0$.

To any set of messages $\{\mathtt{m}_{ia}, \widehat{\mathtt{m}}_{ai}\}$, we associate the Bethe energy

$$\mathbb{F}^{\mathrm{e}}(\underline{\mathtt{m}}, \underline{\widehat{\mathtt{m}}}) = \sum_{a\in F}\mathbb{F}^{\mathrm{e}}_a(\{\mathtt{m}_{ia}\}_{i\in\partial a}) + \sum_{i\in V}\mathbb{F}^{\mathrm{e}}_i(\{\widehat{\mathtt{m}}_{ai}\}_{a\in\partial i}) - \sum_{(ia)\in E}\mathbb{F}^{\mathrm{e}}_{ia}(\mathtt{m}_{ia}, \widehat{\mathtt{m}}_{ai})\,, \tag{19.82}$$

where the various terms are (see Eq. (14.45)):

$$\begin{aligned}
\mathbb{F}^{\mathrm{e}}_a &= \min_{\underline{x}_{\partial a}}\left[E_a(\underline{x}_{\partial a}) + \sum_{j\in\partial a}\mathtt{m}_{ia}(x_i)\right]\,, \qquad \mathbb{F}^{\mathrm{e}}_i = \min_{x_i}\Big[\sum_{a\in\partial i}\widehat{\mathtt{m}}_{ai}(x_i)\Big]\,,\\
\mathbb{F}^{\mathrm{e}}_{ia} &= \min_{x_i}\left[\mathtt{m}_{ia}(x_i) + \widehat{\mathtt{m}}_{ai}(x_i)\right]\,.
\end{aligned} \tag{19.83}$$

Having set up the message passing algorithm and the associated energy functional, we can repeat the program developed in the previous Sections. In particular, in analogy with Assumption 1, we have the following

Assumption 4 *There exist exponentially many quasi-solutions* $\{\underline{\mathtt{m}}^n\}$ *of min-sum equations. The number of such solutions with Bethe energy* $\mathbb{F}^{\rm e}(\underline{\mathtt{m}}^n) \approx N\epsilon$ *is (to leading exponential order)* $\exp\{N\Sigma^{\rm e}(\epsilon)\}$*, where* $\Sigma^{\rm e}(\epsilon)$ *is the* ***energetic complexity function****.*

In order to estimate $\Sigma^{\rm e}(\epsilon)$, we introduce an auxiliary graphical model, whose variables are the min-sum messages $\{\mathtt{m}_{ia}, \widehat{\mathtt{m}}_{ai}\}$. These are forced to satisfy (within some accuracy) the min-sum equations (19.80), (19.81). Each solution is given a weight $e^{-\mathtt{y}\mathbb{F}^{\rm e}(\underline{\mathtt{m}},\underline{\widehat{\mathtt{m}}})}$, with $\mathtt{y} \in \mathbb{R}$. The corresponding distribution is:

$$\mathsf{P}_{\mathtt{y}}(\underline{\mathtt{m}}, \underline{\widehat{\mathtt{m}}}) = \frac{1}{\Xi(\mathtt{y})} \prod_{a\in F} \Psi_a(\{\mathtt{m}_{ja}, \widehat{\mathtt{m}}_{ja}\}_{j\in\partial a}) \prod_{i\in V} \Psi_i(\{\mathtt{m}_{ib}, \widehat{\mathtt{m}}_{ib}\}_{b\in\partial i}) \prod_{(ia)\in E} \Psi_{ia}(\mathtt{m}_{ia}, \widehat{\mathtt{m}}_{ia})\,, \tag{19.84}$$

where:

$$\Psi_a = \prod_{i\in\partial a} \mathbb{I}\left(\widehat{\mathtt{m}}_{ai} = \hat{\mathsf{f}}^{\rm e}_a\left(\{\mathtt{m}_{ja}\}_{j\in\partial a\setminus i}\right)\right) \;\; e^{-\mathtt{y}\mathbb{F}^{\rm e}_a(\{\mathtt{m}_{ja}\}_{j\in\partial a})}\,, \tag{19.85}$$

$$\Psi_i = \prod_{a\in\partial i} \mathbb{I}\left(\mathtt{m}_{ia} = \mathsf{f}^{\rm e}_i\left(\{\widehat{\mathtt{m}}_{bi}\}_{b\in\partial i\setminus a}\right)\right) \;\; e^{-\mathtt{y}\mathbb{F}^{\rm e}_i(\{\widehat{\mathtt{m}}_{bi}\}_{b\in\partial i})}\,, \tag{19.86}$$

$$\Psi_{ia} = e^{\mathtt{y}\mathbb{F}^{\rm e}_{ia}(\mathtt{m}_{ia},\widehat{\mathtt{m}}_{ai})}\,. \tag{19.87}$$

Since the auxiliary graphical model is again locally tree-like, we can hope to derive asymptotically exact results through belief propagation. Messages of the auxiliary problem, to be denoted as $Q_{ia}(\,\cdot\,)$, $\widehat{Q}_{ai}(\,\cdot\,)$, are distributions over the min-sum messages. The $\mathsf{SP}(\mathtt{y})$ equations are obtained by further making the independence assumption (19.27).

The reader has certainly noticed that the whole procedure is extremely close to our study in Sec. 19.2.2. We can apply our previous analysis verbatim to derive the $\mathsf{SP}(\mathtt{y})$ update equations. The only step that requires some care is the formulation of the proper analog of Lemma 19.3. This becomes:

Lemma 19.6 *Assume that* $\mathtt{m}_{ia}(x_i) + \widehat{\mathtt{m}}_{ai}(x_i) < \infty$ *for at least one value of* $x_i \in \mathcal{X}$*. If* $\mathtt{m}_{ia} = \mathsf{f}^{\rm e}_i(\{\widehat{\mathtt{m}}_{bi}\}_{b\in\partial i\setminus a})$*, then*

$$\mathbb{F}^{\rm e}_i - \mathbb{F}^{\rm e}_{ia} = u_{ia}(\{\widehat{\mathtt{m}}_{bi}\}_{b\in\partial i\setminus a}) \equiv \min_{x_i}\Big\{\sum_{b\in\partial i\setminus a} \widehat{\mathtt{m}}_{bi}(x_i)\Big\}\,. \tag{19.88}$$

Analogously, if $\widehat{\mathtt{m}}_{ai} = f^{\rm e}_a(\{\mathtt{m}_{ja}\}_{j\in\partial a\setminus i})$*, then*

$$\mathbb{F}^{\rm e}_a - \mathbb{F}^{\rm e}_{ia} = \hat{u}_{ai}(\{\mathtt{m}_{ja}\}_{j\in\partial a\setminus i}) \equiv \min_{\underline{x}_{\partial a}}\Big\{E_a(\underline{x}_{\partial a}) + \sum_{k\in\partial a\setminus i} \mathtt{m}_{ka}(x_k)\Big\}\,. \tag{19.89}$$

Using this lemma, the same derivation as in Sec. 19.2.2 leads to

Proposition 19.7 *The* $\mathsf{SP}(\mathtt{y})$ *equations are (with the shorthands* $\{\widehat{\mathtt{m}}_{bi}\}$ *for* $\{\widehat{\mathtt{m}}_{bi}\}_{b\in\partial i\setminus a}$ *and* $\{\mathtt{m}_{ja}\}$ *for* $\{\mathtt{m}_{ja}\}_{j\in\partial a\setminus i}$*):*

$$Q_{ia}(\mathtt{m}_{ia}) \cong \sum_{\{\widehat{\mathtt{m}}_{bi}\}} \mathbb{I}\left(\mathtt{m}_{ia} = g_i^{\mathrm{e}}(\{\widehat{\mathtt{m}}_{bi}\})\right) \, e^{-\mathtt{y} u_{ia}(\{\widehat{\mathtt{m}}_{bi}\})} \prod_{b\in\partial i\setminus a} \widehat{Q}_{bi}(\widehat{\mathtt{m}}_{bi}) \,, \quad (19.90)$$

$$\widehat{Q}_{ai}(\widehat{\mathtt{m}}_{ai}) \cong \sum_{\{\mathtt{m}_{ja}\}} \mathbb{I}\left(\widehat{\mathtt{m}}_{ai} = f_a^{\mathrm{e}}(\{\mathtt{m}_{ja}\})\right) \, e^{-\mathtt{y}\hat{u}_{ai}(\{\mathtt{m}_{ja}\})} \prod_{j\in\partial a\setminus i} Q_{ja}(\mathtt{m}_{ja}) \,. \quad (19.91)$$

In the following we shall reserve the name **survey propagation** (SP) for the $\mathtt{y} = \infty$ case of these equations.

19.5.2 *Energetic complexity*

The Bethe free-entropy for the auxiliary graphical model is given by

$$\mathbb{F}^{\mathrm{RSB,e}}(\{Q,\widehat{Q}\}) = \sum_{a\in F} \mathbb{F}_a^{\mathrm{RSB,e}} + \sum_{i\in V} \mathbb{F}_i^{\mathrm{RSB,e}} - \sum_{(ia)\in E} \mathbb{F}_{ia}^{\mathrm{RSB,e}} \,, \quad (19.92)$$

and allows to count the number of min-sum fixed points. The various terms are formally identical to the ones in Eqs. (19.30), (19.31) and (19.32), provided $\mathbb{F}_\cdot(\,\cdot\,)$ is replaced everywhere by $-\mathbb{F}_\cdot^{\mathrm{e}}(\,\cdot\,)$ and $\mathtt{x}$ by $\mathtt{y}$. We reproduce them here for convenience:

$$\mathbb{F}_a^{\mathrm{RSB,e}} = \log\left\{ \sum_{\{\mathtt{m}_{ia}\}} e^{-\mathtt{y}\mathbb{F}_a^{\mathrm{e}}(\{\mathtt{m}_{ia}\})} \prod_{i\in\partial a} Q_{ia}(\mathtt{m}_{ia}) \right\} , \quad (19.93)$$

$$\mathbb{F}_i^{\mathrm{RSB,e}} = \log\left\{ \sum_{\{\widehat{\mathtt{m}}_{ai}\}} e^{-\mathtt{y}\mathbb{F}_i^{\mathrm{e}}(\{\widehat{\mathtt{m}}_{ai}\})} \prod_{a\in\partial i} \widehat{Q}_{ai}(\widehat{\mathtt{m}}_{ai}) \right\} , \quad (19.94)$$

$$\mathbb{F}_{ia}^{\mathrm{RSB,e}} = \log\left\{ \sum_{\mathtt{m}_{ia},\widehat{\mathtt{m}}_{ai}} e^{-\mathtt{y}\mathbb{F}_{ia}^{\mathrm{e}}(\mathtt{m}_{ia},\widehat{\mathtt{m}}_{ai})} Q_{ia}(\mathtt{m}_{ia})\widehat{Q}_{ai}(\widehat{\mathtt{m}}_{ai}) \right\} . \quad (19.95)$$

Assuming that the Bethe free-entropy gives the correct free-entropy of the auxiliary model, the energetic complexity function $\Sigma^{\mathrm{e}}(\epsilon)$ can be computed from $\mathbb{F}^{\mathrm{RSB,e}}(\mathtt{y})$ through the Legendre transform: in the large N limit we expect $\mathbb{F}^{\mathrm{RSB,e}}(\{Q,\widehat{Q}\}) = N\mathfrak{F}^{\mathrm{e}}(\mathtt{y}) + o(N)$ where

$$\mathfrak{F}^{\mathrm{e}}(\{Q,\widehat{Q}\}) = \Sigma^{\mathrm{e}}(\epsilon) - \mathtt{y}\epsilon \,, \qquad \frac{\partial\Sigma^{\mathrm{e}}}{\partial\epsilon} = \mathtt{y} \,. \quad (19.96)$$

Finally, the 1RSB population dynamics algorithm can be used to sample -approximately- the SP($\mathtt{y}$) messages in random graphical models.

19.5.3 *Constraint satisfaction and binary variables*

In Sec. 14.3.3 we noticed that the min-sum messages simplify significantly when one deals with constraint satisfaction problems. In such problems, the energy function takes the form $E(\underline{x}) = \sum_a E_a(\underline{x}_{\partial a})$, where $E_a(\underline{x}_{\partial a}) = 0$ if constraint a is satisfied by the assignment $\underline{x}$, and $E_a(\underline{x}_{\partial a}) = 1$ otherwise. As discussed in

Sec. 14.3.3 the min-sum equations then admit solutions with $\widehat{\mathtt{m}}_{ai}(x_i) \in \{0,1\}$. Furthermore, one does not need to keep track of the variable-to-function node messages $\mathtt{m}_{ia}(x_i)$, but only of their 'projection' on $\{0,1\}$.

In other words, in constraint satisfaction problems the min-sum messages take $2^{|\mathcal{X}|}-1$ possible values (the all-1 message cannot appear). As a consequence, the $\mathsf{SP}(\mathtt{y})$ messages $\widehat{Q}_{ai}(\,\cdot\,)$ and $Q_{ia}(\,\cdot\,)$ simplify considerably: they are points in the $(2^{|\mathcal{X}|}-1)$-dimensional simplex.

If the min-sum messages are interpreted in terms of warnings, as we did in Sec. 14.3.3, then $\mathsf{SP}(\mathtt{y})$ messages keep track of the warnings' statistics (over pure states). One can use this interpretation to derive directly the $\mathsf{SP}(\mathtt{y})$ update equations without going through the whole 1RSB formalism. Let us illustrate this approach on the important case of binary variables $|\mathcal{X}| = 2$.

The min-sum messages $\widehat{\mathtt{m}}$ and $\mathtt{m}$ (once projected) can take three values: $(\widehat{\mathtt{m}}(0), \widehat{\mathtt{m}}(1)) \in \{(0,1),(1,0),(0,0)\}$. We shall denote them respectively as $\mathtt{0}$ (interpreted as a warning: "take value 0"), $\mathtt{1}$ (interpreted as a warning: "take value 1") and $*$ (interpreted as a warning:"you can take any value"). Warning propagation (WP) can be described in words as follows.

Consider the message from variable node i to function node a. This depends on all the messages to i from function nodes $b \in \partial i \setminus a$. Suppose that $\widehat{n}_{\mathtt{0}}$ (respectively, $\widehat{n}_{\mathtt{1}}$, $\widehat{n}_{*}$) of these messages are of type $\mathtt{0}$ (resp. $\mathtt{1}$, $*$) for $i \in \partial a$. If $\widehat{n}_{\mathtt{0}} > \widehat{n}_{\mathtt{1}}$, i sends to a a $\mathtt{0}$ message. If $\widehat{n}_{\mathtt{1}} > \widehat{n}_{\mathtt{0}}$, it sends to a a $\mathtt{1}$ message. If $\widehat{n}_{\mathtt{1}} = \widehat{n}_{\mathtt{0}}$, it send to a a $*$ message. The 'number of contradictions' among the messages that it receives is: $\mathbb{F}^{\rm e}_i - \mathbb{F}^{\rm e}_{ia} = u_{ia} = \min(\widehat{n}_{\mathtt{1}}, \widehat{n}_{\mathtt{0}})$.

Now consider the message from function node a to variable node i. It depends on the ones coming from neighboring variables $j \in \partial a \setminus i$. Partition the neighbors into subsets $\mathcal{P}_*, \mathcal{P}_{\mathtt{0}}, \mathcal{P}_{\mathtt{1}}$, whereby $\mathcal{P}_{\mathtt{m}}$ is the set of indices j such that $\mathtt{m}_{ja} = \mathtt{m}$. For each value of $x_i \in \{0,1\}$, the algorithm computes the minimal value of $E_a(\underline{x}_{\partial a})$ such that the variables in $\mathcal{P}_{\mathtt{0}}$ (respectively, $\mathcal{P}_{\mathtt{1}}$) are fixed to 0 (resp. to 1). More explicitly, let us define a function $\Delta_{\mathcal{P}}(x_i)$ as follows:

$$\Delta_{\mathcal{P}}(x_i) = \min_{\{x_j\}_{j\in\mathcal{P}_*}} E_a(x_i, \{x_j\}_{j\in\mathcal{P}_*}, \{x_k = 0\}_{k\in\mathcal{P}_{\mathtt{0}}}, \{x_l = 1\}_{l\in\mathcal{P}_{\mathtt{1}}})\,. \qquad (19.97)$$

The following table then gives the outgoing message $\widehat{\mathtt{m}}_{ai}$ and the number of contradictions at a, $\mathbb{F}^{\rm e}_a - \mathbb{F}^{\rm e}_{ai} = \hat{u}_{ai}$ as a function of the values $\Delta_{\mathcal{P}}(0)$ and $\Delta_{\mathcal{P}}(1)$:

$\Delta_{\mathcal{P}}(0)$	$\Delta_{\mathcal{P}}(1)$	$\widehat{\mathtt{m}}_{ai}$	$\hat{u}_{ai}$
0	0	$*$	0
0	1	$\mathtt{0}$	0
1	0	$\mathtt{1}$	0
1	1	$*$	1

Having established the WP update rules, it is immediate to write the $\mathsf{SP}(\mathtt{y})$ equations. Consider a node, and one of its neighbors to which it sends messages. For each possible configuration of incoming warnings on the node, denoted by $\mathtt{input}$, we

found the rules to compute the outgoing warning $\mathtt{output} = \widehat{\mathtt{OUT}}(\mathtt{input})$ and the number of contradictions $\delta\mathbb{F}^{\mathrm{e}}(\mathtt{input})$. $\mathsf{SP}(\mathtt{y})$ messages are distributions over $(\mathtt{0},\mathtt{1},*)$: $(Q_{ia}(\mathtt{0}), Q_{ia}(\mathtt{1}), Q_{ia}(*))$ and $(\widehat{Q}_{ai}(\mathtt{0}), \widehat{Q}_{ai}(\mathtt{1}), \widehat{Q}_{ai}(*))$. Notice that these messages are only marginally more complicated than ordinary BP messages. Let $\mathbb{P}(\mathtt{input})$ denote the probability of a given input assuming independent warnings with distribution $Q_{ia}(\,\cdot\,)$ (respectively, $\widehat{Q}_{ai}(\,\cdot\,)$). The probability of an outgoing message $\mathtt{output} \in \{\mathtt{0},\mathtt{1},*\}$ is then:

$$\mathbb{P}(\mathtt{output}) \cong \sum_{\mathtt{input}} \mathbb{P}(\mathtt{input})\mathbb{I}(\widehat{\mathtt{OUT}}(\mathtt{input}) = \mathtt{output}) e^{-\mathtt{y}\delta\mathbb{F}^{\mathrm{e}}(\mathtt{input})}\,. \quad (19.98)$$

Depending whether the node we are considering is a variable or function node, this probability distribution corresponds to the outgoing message $Q_{ia}(\,\cdot\,)$ or $\widehat{Q}_{ai}(\,\cdot\,)$.

It can be shown that the Bethe energy (19.83) associated with a given fixed point of the WP equations coincides with the total number of contradictions. This is expressed as the number of contradictions at function nodes, plus those at variable nodes, minus the number of edges (i,a) such that the warning in direction $a \to i$ contradicts the one in direction $i \to a$ (the last term avoids double counting). It follows that the Bethe free-entropy of the auxiliary graphical model $\mathbb{F}^{\mathrm{RSB,e}}(\mathtt{y})$ weights each WP fixed point depending on its number of contradictions, as it should.

19.5.4 *XORSAT again*

Let us know apply the $\mathsf{SP}(\mathtt{y})$ formalism to random K-XORSAT instances. We let the energy function $E(\underline{x})$ count the number of unsatisfied linear equations:

$$E_a(\underline{x}_{\partial a}) = \begin{cases} 0 & \text{if } x_{i_1(a)} \oplus \cdots \oplus x_{i_K(a)} = b_a, \\ 1 & \text{otherwise.} \end{cases} \quad (19.99)$$

The simplifications discussed in the previous subsection apply to this case. The 1RSB population dynamics algorithm can be used to compute the free-entropy density $\mathfrak{F}^{\mathrm{e}}(\mathtt{y})$. Here we limit ourselves to describing the results of this calculation for the case $K = 3$.

Let us stress that the problem we are considering here is different from the one investigated in Section 19.3. While there we were interested in the uniform measure over solutions (thus focusing on the satisfiable regime $\alpha < \alpha_{\mathrm{s}}(K)$), here we are estimating the minimum number of unsatisfied constraints (which is most interesting in the unsatisfiable regime $\alpha > \alpha_{\mathrm{s}}(K)$).

It is easy to show that the $\mathsf{SP}(\mathtt{y})$ equations always admit a solution in which $Q_{ia}(*) = 1$ for all (i,a), indicating that the min-sum equations have a unique solution. This corresponds to a density evolution fixed point whereby $Q(*) = 1$ with probability 1, yielding $\mathfrak{F}^{\mathrm{e}}(\mathtt{y})$ independent of $\mathtt{y}$. For $\mathtt{y}$ smaller than an α-dependent threshold $\mathtt{y}^*(\alpha)$, this is the only solution we find. For larger values of $\mathtt{y}$, the $\mathsf{SP}(\mathtt{y})$ equations have a non-trivial solution. Fig. 19.4 shows the result for the free-entropy density $\mathfrak{F}^{\mathrm{e}}(\mathtt{y})$, for three values of α.

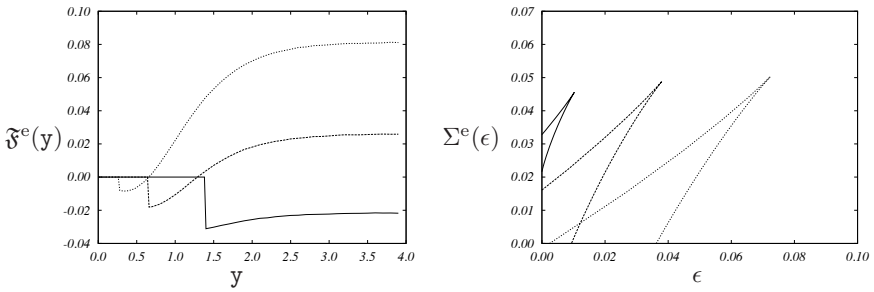

FIG. 19.4. Random 3-XORSAT at $\alpha = 0.87$, 0.97 and 1.07. Recall that, for $K = 3$, $\alpha_{\rm d}(K) \approx 0.818$ and $\alpha_{\rm s}(K) \approx 0.918$. Left frame: Free-entropy density $\mathfrak{F}^{\rm e}(\mathtt{y})$ as a function of $\mathtt{y}$, obtained using the population dynamics algorithm, with $N = 2 \cdot 10^4$ and $t = 5 \cdot 10^3$ (α increases from bottom to top). Right frame: Complexity $\Sigma^{\rm e}(\epsilon)$ as a function of energy density (equal to the number of violated constraints per variable). α increases from left to right.

Above this threshold density evolution converges to a 'non-trivial' 1RSB fixed point. The complexity functions $\Sigma^{\rm e}(\epsilon)$ can be deduced by Legendre transform, cf. Eq. (19.96), which requires differentiating $\mathfrak{F}^{\rm e}(\mathtt{y})$ and plotting $(\epsilon, \Sigma^{\rm e})$ in parametric form. The derivative can be computed numerically in a number of ways:

1. Compute analytically the derivative of $\mathbb{F}^{\rm RSB,e}(\mathtt{y})$ with respect to $\mathtt{y}$. This turns out to be a functional of the fixed point distributions of Q, $\widehat{Q}$, and can therefore be easily evaluated.
2. Fit the numerical results for the function $\mathfrak{F}^{\rm e}(\mathtt{y})$ and differentiate the fitting function
3. Approximate the derivative as difference at nearby values of $\mathtt{y}$.

In the present case we followed the second approach using the parametric form $\mathfrak{F}^{\rm fit}(\mathtt{y}) = a + b\, e^{-\mathtt{y}} + c\, e^{-2\mathtt{y}} + d\, e^{-3\mathtt{y}}$. As shown in Fig. 19.4 the resulting parametric curve $(\epsilon, \Sigma^{\rm e})$ is multiple valued (this is a consequence of the fact that $\mathfrak{F}^{\rm e}(\mathtt{y})$ is not concave). Only the concave part of $\mathfrak{F}^{\rm e}(\mathtt{y})$ is retained as physically meaningful. Indeed the convex branch is 'unstable' (in the sense that further RSB would be needed) and it is not yet understood whether it has any meaning.

For $\alpha \in [\alpha_{\rm d}(K), \alpha_{\rm s}(K)[$, $\Sigma^{\rm e}(\epsilon)$ remains positive down to $\epsilon = 0$. The intercept $\Sigma^{\rm e}(\epsilon = 0)$ coincides with the complexity of clusters of SAT configurations, as computed in Ch. 18 (see Theorem 18.2). For $\alpha > \alpha_{\rm s}(K)$ (UNSAT phase) $\Sigma^{\rm e}(\epsilon)$ vanishes at $\epsilon_{\rm gs}(K, \alpha) > 0$. The energy density $\epsilon_{\rm gs}(K, \alpha)$ is the minimal fraction of violated equations, in a random XORSAT linear system. Notice that $\Sigma^{\rm e}(\epsilon)$ is not defined above a second energy density $\epsilon_{\rm d}(K, \alpha)$. This indicates that we should take $\Sigma^{\rm e}(\epsilon) = -\infty$ there: above $\epsilon_{\rm d}(K, \alpha)$ one recovers a simple problem with a unique Bethe measure.

Figure 19.5 shows the values of $\epsilon_{\rm gs}(K, \alpha)$ and $\epsilon_{\rm d}(K, \alpha)$ as functions of α for $K = 3$ (random 3-XORSAT).

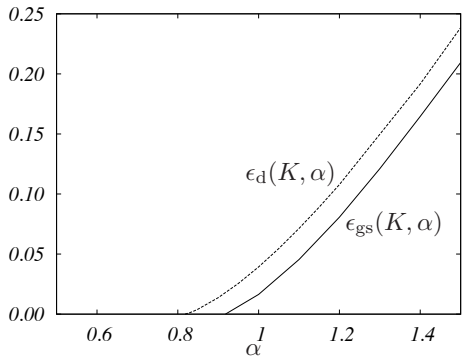

FIG. 19.5. Asymptotic ground state energy (= minimal number of violated constraints) per variable $\epsilon_{\rm gs}(K,\alpha)$ for random K = 3-XORSAT formulae. $\epsilon_{\rm gs}(K,\alpha)$ vanishes for $\alpha < \alpha_{\rm s}(K)$. The dashed line $\epsilon_{\rm d}(K,\alpha)$ is the highest energy density e such that configurations with $E(\underline{x}) < Ne$ are clustered. It vanishes for $\alpha < \alpha_{\rm d}(K)$.

19.6 The nature of 1RSB phases

In the last sections we discussed how to compute the complexity function $\Sigma(\phi)$ (or its 'zero temperature' version, the energetic complexity $\Sigma^{\rm e}(\epsilon)$). Here we want to come back to the problem of determining some qualitative properties of the measure $\mu(\,\cdot\,)$ for random graphical models, on the basis of its decomposition into extremal Bethe measures:

$$\mu(\underline{x}) = \sum_{n\in\mathsf{E}} w_n \mu^n(\underline{x})\,. \tag{19.100}$$

Assumptions 2 and 3 imply that, in this decomposition, we introduce a negligible error if we drop all the states n but the ones with free-entropy $\phi_n \approx \phi_*$, where

$$\phi_* = \operatorname{argmax}\{\phi + \Sigma(\phi) :\ \Sigma(\phi) \geq 0\}\ . \tag{19.101}$$

In general, $\Sigma(\phi)$ is strictly positive and continuous in an interval $[\phi_{\rm min}, \phi_{\rm max}]$ with $\Sigma(\phi_{\rm max}) = 0$, and

$$\Sigma(\phi) = \mathtt{x}_*(\phi_{\rm max} - \phi) + O((\phi_{\rm max} - \phi)^2)\,, \tag{19.102}$$

for ϕ close to $\phi_{\rm max}$.

It turns out that the decomposition (19.100) has different properties depending on the result of the optimization (19.101). One can distinguish two phases (see Fig. 19.6): d1RSB (dynamic one-step replica symmetry breaking) when the max is achieved in the interior of $[\phi_{\rm min}, \phi_{\rm max}]$ and, as a consequence $\Sigma(\phi_*) > 0$; s1RSB (static one-step replica symmetry breaking) when the max is achieved at $\phi_* = \phi_{\rm max}$ and therefore $\Sigma(\phi_*) = 0$ (this case occurs iff $\mathtt{x}_* \leq 1$).

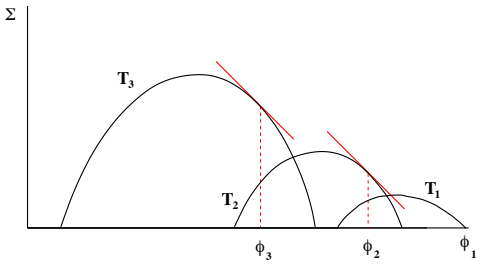

FIG. 19.6. A sketch of the complexity Σ versus free-entropy-density ϕ in a finite-temperature problem with 1RSB phase transition, at three temperatures $T_1 < T_2 < T_3$. A random configuration $\underline{x}$ with distribution $\mu(\underline{x})$ is found with high probability in a cluster of free-entropy-density ϕ_1, ϕ_2, ϕ_3 respectively. T_2 and T_3 are above the condensation transition: ϕ_2, ϕ_3 are the points where $\partial\Sigma/\partial\phi = -1$. T_1 is below the condensation transition: ϕ_1 is the largest value of ϕ where Σ is positive.

19.6.1 *Dynamical 1RSB*

Assume $\Sigma_* = \Sigma(\phi_*) > 0$. Then we can restrict the sum (19.100) to those states n such that $\phi_n \in [\phi_* - \varepsilon, \phi_* + \varepsilon]$, if we allow for an exponentially small error. To the leading exponential order there are $e^{N\Sigma_*}$ such states whose weights are $w_n \in [e^{-N(\Sigma_*+\varepsilon')}, e^{-N(\Sigma_*-\varepsilon')}]$.

Different states are expected to have essentially disjoint support. By this we mean that there exists subsets $\{\Omega_n\}_{n\in\mathsf{E}}$ of the configuration space $\mathcal{X}^N$ such that, for any $m \in \mathsf{E}$

$$\mu^m(\Omega_m) \approx 1\,, \qquad \sum_{n\in\mathsf{E}\setminus m} w_n \mu^n(\Omega_m) \approx 0\,. \tag{19.103}$$

Further, different states are separated by 'large free-energy barriers.' This means that one can choose the above partition in such a way that only an exponentially small (in N) fraction of the probability measure is on its boundaries.

This structure has two important consequences:

Glassy dynamics. Let us consider a local Markov Chain dynamics that satisfies detailed balance with respect to the measure $\mu(\,\cdot\,)$. As an example we can consider the Glauber dynamics introduced in Ch. 4 (in order to avoid trivial reducibility effects, we can assume in this discussion that the compatibility functions $\psi_a(\underline{x}_{\partial a})$ are bounded away from 0).

Imagine initiating the dynamics at time 0 with an equilibrated configuration $\underline{x}(0)$ distributed according to $\mu(\,\cdot\,)$. This is essentially equivalent to picking a state n uniformly at random among the typical ones, and then sampling $\underline{x}(0)$ from $\mu^n(\,\cdot\,)$. Because of the exponentially large barriers, the dynamics will stay confined in Ω_n for an exponentially large time, and equilibrate among states only on larger time scales.

This can be formalized as follows. Denote by $D(\underline{x},\underline{x}')$ the Hamming distance in $\mathcal{X}^N$. Take two i.i.d. configuration with distribution μ and let Nd_0 be the expectation value of their Hamming distance. Analogously take two i.i.d. configuration with distribution μ^n, and let Nd_1 be the expectation value of their Hamming distance. When the state n is chosen randomly with distribution w_n, we expect d_1 not to depend on the state n asymptoticaly for large sizes. Furthermore: $d_1 < d_0$. Then we can consider the (normalized) expected Hamming distance between configurations at time t in Glauber dynamics $d(t) = \langle D(\underline{x}(0),\underline{x}(t))\rangle/N$. For any $\varepsilon < d_0 - d_1$, the correlation time $\tau(\varepsilon) \equiv \inf\{t :\ d(t) \geq d_0 - \varepsilon\}$ is expected to be exponentially large in N

Short-range correlations in finite-dimensional projections. We motivated the 1RSB cavity method with the emergence of long-range correlations due to decomposition of $\mu(\,\cdot\,)$ into many extremal Bethe measures. Surprisingly, such correlations cannot be detected by probing a bounded (when $N \to \infty$) number of variables. More precisely, if $i(1),\dots,i(k) \in \{1,\cdots,N\}$ are uniformly random variable indices, then, in the d1RSB phase:

$$\mathbb{E}|\langle f_1(x_{i(1)})f_2(x_{i(2)})\cdots f_k(x_{i(k)})\rangle - \langle f_1(x_{i(1)})\rangle\langle f_2(x_{i(2)})\rangle\cdots\langle f_k(x_{i(k)})\rangle| \stackrel{N\to\infty}{\to} 0\,.$$

(Here $\langle\,\cdot\,\rangle$ denote the expectation with respect to the measure μ, and $\mathbb{E}$ the expectation with respect to the graphical model in a random ensemble). This finding can be understood intuitively as follows. If there are long range correlations among subsets of k variables, then it must be true that conditioning on the values of $k-1$ of them changes the marginal distribution of the k-th one. On the other hand, we think that long range correlations arise because far apart variables 'know' that the whole system is in the same state n. But conditioning on a bounded number $(k-1)$ of variables cannot select in any significant way among the $e^{N\Sigma_*}$ relevant states, and thus cannot change the marginal of the k-th one.

An alternative argument makes use of the observation that, if $\underline{x}^{(1)}$ and $\underline{x}^{(2)}$ are two i.i.d. configurations with distribution $\mu(\,\cdot\,)$, then their distance $D(\underline{x}^{(1)},\underline{x}^{(2)})$ concentrates in probability. This is due to the fact that the two configurations will be, with high probability, in different states $n_1 \neq n_2$ (the probability of $n_1 = n_2$ being $e^{-N\Sigma_*}$), whose distance depends weakly on the states couple.

Let us finally notice that the absence of long range correlations among bounded subset of variables is related to the observation that $\mu(\,\cdot\,)$ is itself a Bethe measure (although a non-extremal one) in a d1RSB phase, cf. Sec. 19.4.1. Indeed, each BP equation involves a bounded subset of the variables and can be violated only because of correlations among them.

As we shall discuss in Sec. 22.1.2, long range correlations in a d1RSB phase can be probed through more sophisticated "point-to-set" correlation functions.

19.6.2 *Static 1RSB*

In this case the decomposition (19.100) is dominated by a few states of near-to-maximal free-entropy $\phi_n \approx \phi_{\max}$. If we 'zoom' near the edge by letting $\phi_n =$

$\phi_{\max} + s_n/N$, then the 'free-entropy shifts' s_n form a point process with density $\exp(-\mathtt{x}_* s)$.

The situation is analogous to the one we found in the random energy model for $T < T_{\rm c}$. Indeed it is expected that the weights $\{w_n\}$ converge to the same universal Poisson-Dirichlet process found there, and to depend on the model details only through the parameter $\mathtt{x}_*$ (we have already discussed this universality using replicas in Ch. 8). In particular, if $\underline{x}^{(1)}$ and $\underline{x}^{(2)}$ are two i.i.d. replicas with distribution μ, and n_1, n_2 are the states they belong to, then the probability for them to belong to the same state is

$$\mathbb{E}\left\{\mathbb{P}_\mu(n_1 = n_2)\right\} = \mathbb{E}\left\{\sum_{n\in\mathsf{E}} w_n^2\right\} = 1 - x_* \,. \tag{19.104}$$

Here $\mathbb{E}$ denote expectation with respect to the graphical model distribution.

As a consequence, the distance $D(\underline{x}^{(1)}, \underline{x}^{(2)})$ between two i.i.d. replicas does not concentrate (the overlap distribution is non-trivial). This in turn can only be true if the two-point correlation function does not vanish at large distances. Long-range correlations of this type make BP break down. The original graphical model $\mu(\,\cdot\,)$ is no longer a Bethe measure: its local marginals cannot be described in terms of a set of messages. The 1RSB description, according to which $\mu(\,\cdot\,)$ is a convex combination of Bethe measures, is unavoidable.

At this point we are left with a puzzle. How to circumvent the argument given in Section 19.4.1 that, if the 'correct' weight $\mathtt{x} = 1$ is used, then the marginals as computed within 1RSB still satisfy BP equations? The conundrum is that, within a $\mathsf{s1RSB}$ phase, the parameter $\mathtt{x} = 1$ is *not* the correct one to be used in the 1RSB cavity equations (although it is the correct one to weight states). In order to explain this, let us first notice that, if the complexity is convex and behaves as in Eq. (19.102) near its edge, with a slope $-\mathtt{x}_* > -1$, then the optimization problem (19.101) has the same result as

$$\phi_* = \operatorname{argmax}\left\{\mathtt{x}\phi + \Sigma(\phi) :\ \Sigma(\phi) \geq 0\right\} \,. \tag{19.105}$$

for any $\mathtt{x} \geq \mathtt{x}_*$. Therefore, in the 1RSB cavity equations we could in principle use any value of $\mathtt{x}$ larger or equal to $\mathtt{x}_*$ (this would select the same states). However, the constraint $\Sigma(\phi) \geq 0$ cannot be enforced locally and does not show up in the cavity equations. If one performs the computation of Σ within the cavity method using a value $\mathtt{x} > \mathtt{x}_*$, then one finds a negative value of Σ which must be rejected (it is believed to be related to the contribution of some exponentially rare instances). Therefore, in order to ensure that one studies the interval of ϕ such that $\Sigma(\phi) \geq 0$, one must *impose* $\mathtt{x} \leq \mathtt{x}_*$ in the cavity method. In order to select the states with free-entropy density $\phi_{\max}$, we must thus choose the Parisi parameter that corresponds to $\phi_{\max}$, namely $\mathtt{x} = \mathtt{x}_*$.

19.6.3 *When does 1RSB fail?*

The 1RSB cavity method is a powerful tool, but does not always provide correct answers, even for locally tree-like models, in the large system limit. The

main assumption of the 1RSB approach is that, once we pass to the auxiliary graphical model (which 'enumerates' BP fixed points) a simple BP procedure is asymptotically exact. In other words, the auxiliary problem has a simple 'replica symmetric' structure and no glassy phase. This is correct in some cases, such as random XORSAT or SAT close to their SAT-UNSAT threshold, but it may fail in others.

A mechanism leading to a failure of the 1RSB approach is that the auxiliary graphical model is incorrectly described by BP. This may happen because the auxiliary model measure decomposes in many Bethe states. In such a case, one should introduce a second auxiliary model, dealing with the multiplicity of BP fixed points of the first one. This is usually referred to as 'two-step replica symmetry breaking' (2RSB). Obviously one can find situations in which it is necessary to iterate this construction, leading to a R-th level auxiliary graphical model (R-RSB). Continuous (or full) RSB corresponds to the large-R limit.

While such developments are conceptually clear (at least from an heuristic point of view), they are technically challenging. So far limited results have been obtained beyond 1RSB. For a brief survey, we refer to Ch. 22.

Appendix: $\mathsf{SP}(\mathtt{y})$ equations for XORSAT

This appendix provides technical details on the 1RSB treatment of random K-XORSAT, within the 'energetic' formalism. The results of this approach were discussed in Sec. 19.5.4. In particular we will derive the behavior of the auxiliary free-entropy $\mathfrak{F}^{\rm e}(\mathtt{y})$ at large $\mathtt{y}$, and deduce the behavior of the complexity $\Sigma^{\rm e}(\epsilon)$ at small ϵ. This section can be regarded as an exercise in applying the $\mathsf{SP}(\mathtt{y})$ formalism. We shall skip many details and just give the main intermediate results of the computation.

XORSAT is a constraint satisfaction problems with binary variables. We can thus apply the simplified method of Sec. 19.5.3. The projected min-sum messages can take three values: $\mathtt{0}$, $\mathtt{1}$, $*$. Exploiting the symmetry of XORSAT between $\mathtt{0}$ and $\mathtt{1}$, $\mathsf{SP}(\mathtt{y})$ messages can be parametrized by a single number, e.g. by the sum of their weights on $\mathtt{0}$ and $\mathtt{1}$. We will therefore write: $Q_{ia}(\mathtt{0}) = Q_{ia}(\mathtt{1}) = \zeta_{ia}/2$ (thus implying $Q_{ia}(*) = 1-\zeta_{ia}$), and $\widehat{Q}_{ai}(\mathtt{0}) = \widehat{Q}_{ai}(\mathtt{1}) = \eta_{ai}/2$ (whence $\widehat{Q}_{ai}(*) = 1-\eta_{ai}$).

In terms of these variables, the $\mathsf{SP}(\mathtt{y})$ equation at function node a reads:

$$\eta_{ai} = \prod_{j\in\partial a\setminus i} \zeta_{ja}\,. \tag{19.106}$$

The $\mathsf{SP}(\mathtt{y})$ equation at variable node i is a bit more complicated. Let us consider all the $|\partial i|-1$ incoming messages $\widehat{Q}_{bi}$, $b\in\partial i\setminus a$. Each of them is parameterized by a number η_{bi}. We let $\underline{\eta} = \{\eta_{bi},\ b\in\partial i\setminus a\}$ and define the function $B_q(\underline{\eta})$ as follows:

$$B_q(\underline{\eta}) = \sum_{S\subset\{\partial i\setminus a\}} \mathbb{I}(|S|=q) \prod_{b\in\partial i\setminus\{S\cup\{a\}\}} (1-\eta_{bi}) \prod_{c\in S}\eta_{cj}\,. \tag{19.107}$$

Let $A_{q,r}(\underline{\eta}) = B_{q+r}(\underline{\eta})\binom{q+r}{q}2^{-(q+r)}$. After some thought one obtains the update equation:

$$\zeta_{ia} = \frac{2\sum_{q=0}^{|\partial i|-2}\sum_{r=q+1}^{|\partial i|-1} A_{q,r}(\underline{\eta})e^{-\mathtt{y}q}}{\sum_{q=0}^{\lfloor(|\partial i|-1)/2\rfloor} A_{q,q}(\underline{\eta})e^{-\mathtt{y}q} + 2\sum_{q=0}^{|\partial i|-2}\sum_{r=q+1}^{|\partial i|-1} A_{q,r}(\underline{\eta})e^{-\mathtt{y}q}} \tag{19.108}$$

The auxiliary free-entropy $\mathbb{F}^{\mathrm{RSB,e}}(\mathtt{y})$ has the general form (19.92), with the various contributions expressed as follows in terms of the parameters $\{\zeta_{ia}, \eta_{ai}\}$:

$$e^{\mathbb{F}_a^{\mathrm{RSB,e}}} = 1 - \frac{1}{2}(1-e^{-\mathtt{y}})\prod_{i\in\partial a}\zeta_{ia}\,, \qquad e^{\mathbb{F}_{ai}^{\mathrm{RSB,e}}} = 1 - \frac{1}{2}\eta_{ai}\zeta_{ia}(1-e^{-\mathtt{y}})\,,$$

$$e^{\mathbb{F}_i^{\mathrm{RSB,e}}} = \sum_{q=0}^{d_i}\sum_{r=0}^{d_i-q} A_{q,r}\left(\{\eta_{ai}\}_{a\in\partial i}\right)\; e^{-\mathtt{y}\min(q,r)}\,. \tag{19.109}$$

Let us consider random K-XORSAT instances with constraint density α. Equations (19.106), (19.108) get promoted to distributional relations that determine the asymptotic distribution of η and ζ on a randomly chosen edge (i,a). The 1RSB population dynamics algorithm can be used to approximate these distributions. We encourage the reader to implement it, and obtain a numerical estimate of the auxiliary free-entropy density $\mathfrak{F}^{\mathrm{e}}(\mathtt{y})$.

It turns out that, at large $\mathtt{y}$, one can control the distributions of η, ζ analytically, provided their qualitative behavior satisfies the following assumptions (that can be checked numerically):

- With probability t one has $\eta = 0$, and with probability $1-t$, $\eta = 1-e^{-\mathtt{y}}\hat{\eta}$, where t has a limit in $]0,1[$, and $\hat{\eta}$ converges to a random variable with support on $[0,\infty[$, as $\mathtt{y}\to\infty$.
- With probability s one has $\zeta = 0$, and with probability $1-s$, $\zeta = 1-e^{-\mathtt{y}}\hat{\zeta}$, where s has a limit in $]0,1[$, and $\hat{\zeta}$ converges to a random variable with support on $[0,\infty[$, as $\mathtt{y}\to\infty$.

Under these assumptions, we shall expand the distributional version of Eqs. (19.106), (19.108) keeping terms up to first order in $e^{-\mathtt{y}}$. We shall use $t, s, \hat{\eta}, \hat{\zeta}$ to denote the limit quantities mentioned above.

It is easy to see that t, s must satisfy the equations $(1-t) = (1-s)^{k-1}$ and $s = e^{-K\alpha(1-t)}$. These are identical to Eqs. (19.51) and (19.52), whence $t = 1-\widehat{Q}_*$ and $s = 1-Q_*$.

Equation (19.106) leads to the distributional equation:

$$\hat{\eta} \stackrel{\mathrm{d}}{=} \hat{\zeta}_1 + \cdots + \hat{\zeta}_{K-1}\,, \tag{19.110}$$

where $\hat{\zeta}_1, \ldots, \hat{\zeta}_{K-1}$ are $K-1$ i.i.d. copies of the random variable $\hat{\zeta}$.

The update equation (19.108) is more complicated. There are in general l inputs to a variable node, where l is Poisson with mean $K\alpha$. Let us denote by

m the number of incoming messages with $\eta = 0$. The case $m = 0$ yields $\zeta = 0$ and is taken care of in the relation between t and s. If we condition on $m \geq 1$, the distribution of m is

$$\mathbb{P}(m) = \frac{\lambda^m}{m!} e^{-\lambda} \frac{1}{1 - e^{-\lambda}} \mathbb{I}(m \geq 1) \;, \tag{19.111}$$

where $\lambda = K\alpha(1-t)$. Conditional on m, Eq. (19.108) simplifies as follows:

- If $m = 1$: $\hat{\zeta} \stackrel{\mathrm{d}}{=} \hat{\eta}$.
- If $m = 2$: $\hat{\zeta} = 1$ identically.
- If $m \geq 3$: $\hat{\zeta} = 0$ identically.

The various contributions to the free-entropy (19.38) are given by:

$$\mathrm{f}_{\mathrm{f}}^{\mathrm{RSB,e}} = (1-s)^k \left[-\log 2 + e^{-\mathrm{y}}(1 + K\langle\hat{\zeta}\rangle) \right] + o(e^{-\mathrm{y}}) \,, \tag{19.112}$$

$$\begin{aligned} \mathrm{f}_{\mathrm{v}}^{\mathrm{RSB,e}} = {} & \frac{\lambda^2}{2} e^{-\lambda} \left[-\log 2 + e^{-\mathrm{y}}(1 + 2\langle\hat{\eta}\rangle) \right] \\ & + \sum_{m=3}^{\infty} \frac{\lambda^m}{m!} e^{-\lambda} \left[(1-m)\log 2 + e^{-\mathrm{y}} m (1 + \langle\hat{\eta}\rangle) \right] + o(e^{-\mathrm{y}}) \,, \end{aligned} \tag{19.113}$$

$$\mathrm{f}_{\mathrm{e}}^{\mathrm{RSB,e}} = (1-t)(1-s) \left[-\log 2 + e^{-\mathrm{y}}(1 + \langle\hat{\eta}\rangle + \langle\hat{\zeta}\rangle) \right] + o(e^{-\mathrm{y}}) \;, \tag{19.114}$$

where $\langle\hat{\eta}\rangle$ and $\langle\hat{\zeta}\rangle$ are the expectation values of $\hat{\eta}$ and $\hat{\zeta}$. This gives for the free-entropy density $\mathfrak{F}^{\mathrm{e}}(\mathrm{y}) = \mathrm{f}_{\mathrm{f}}^{\mathrm{RSB,e}} + \alpha \mathrm{f}_{\mathrm{v}}^{\mathrm{RSB,e}} - K\alpha\, \mathrm{f}_{\mathrm{e}}^{\mathrm{RSB,e}} = \Sigma_0 + e^{-\mathrm{y}}\epsilon_0 + o(e^{-\mathrm{y}})$, with:

$$\Sigma_0 = \left[1 - \frac{\lambda}{k} - e^{-\lambda} \left(1 + \frac{k-1}{k} \lambda \right) \right] \log 2 \,, \tag{19.115}$$

$$\epsilon_0 = \frac{\lambda}{k} \left[1 - e^{-\lambda} \left(1 + \frac{k}{2} \lambda \right) \right] \;. \tag{19.116}$$

Taking the Legendre transform, cf. Eq. (19.96), we obtain the following behavior of the energetic complexity as $\epsilon \to 0$:

$$\Sigma^{\mathrm{e}}(\epsilon) = \Sigma_0 + \epsilon \log \frac{\epsilon_0 e}{\epsilon} + o(\epsilon) \;, \tag{19.117}$$

This shows in particular that the ground state energy density is proportional to $(\alpha - \alpha_s)/|\log(\alpha - \alpha_s)|$ close to the SAT-UNSAT transition (when $0 < \alpha - \alpha_s \ll 1$).

Exercise 19.7 In the other extreme, show that at large α one gets $\epsilon_{\mathrm{gs}}(K, \alpha) = \alpha/2 + \sqrt{2\alpha}\epsilon_*(K) + o(\sqrt{\alpha})$, where the positive constant $\epsilon_*(K)$ is the absolute value of the ground state energy of the fully connected K-spin model studied in Sec. 8.2. This indicates that there is no interesting intermediate asymptotic regime between the $M = \Theta(N)$ (discussed in the present chapter) and $M = \Theta(N^{K-1})$ (discussed with the replica method in Ch. 8)

Notes

The cavity method originated as an alternative to the replica approach in the study of the Sherrington-Kirkatrick model (Mézard, Parisi and Virasoro, 1985*b*). The 1RSB cavity method for locally tree-like factor graphs was developed in the context of spin glasses in (Mézard and Parisi, 2001). Its application to zero temperature problems (counting solutions of the min-sum equations), was also first described in the spin glass context in (Mézard and Parisi, 2003). The presentation in this chapter differs in its scope from those work, which were more focused in computing averages over random instances. For a rigorous treatment of the notion of Bethe measure, we refer to (Dembo and Montanari, 2008*b*).

The idea that the 1RSB cavity method is in fact equivalent to applying BP on an auxiliary model appeared in several paper treating the cases of coloring and satisfiability with $\mathtt{y} = 0$ (Parisi, 2002; Braunstein and Zecchina, 2004; Maneva, Mossel and Wainwright, 2005). The treatment presented here generalizes these works, with the important difference that the variables of our auxiliary model are messages rather than node quantities.

The analysis of the $\mathtt{x} = 1$ case is strictly related to the problem of reconstruction on a tree. This has been studied in (Mézard and Montanari, 2006), where the reader will find the proof of Theorem 19.5 and the expression of the free-entropy of exercise 19.6.

The $\mathsf{SP}(\mathtt{y})$ equations for one single instance have been written first in the context of the K-satisfiability problem in (Mézard and Zecchina, 2002), see also (Mézard, Parisi and Zecchina, 2003). The direct derivation of $\mathsf{SP}(\mathtt{y})$ equations in binary variable problems, shown in Sec. 19.5.3, was done originally for satisfiability in (Braunstein, Mézard and Zecchina, 2005), see also (Braunstein and Zecchina, 2004) and (Maneva, Mossel and Wainwright, 2005). The application of the 1RSB cavity method to the random XORSAT problem, and its comparison to the exact results, was done in (Mézard, Ricci-Tersenghi and Zecchina, 2003).

An alternative to the cavity approach followed throughout this book is provided by the replica method of Ch. 8. As we saw, it was first invented in order to treat fully connected models (i.e. models on complete graphs), cf. (Mézard, Parisi and Virasoro, 1987), and subsequently developed in the context of sparse random graphs (Mézard and Parisi, 1985; Dominicis and Mottishaw, 1987; Mottishaw and Dominicis, 1987; Wong and Sherrington, 1988; Goldschmidt and Lai, 1990). The technique was further improved in the paper (Monasson, 1998), that offers a very lucid presentation of the method.